Conceptualising surface water-groundwater exchange in braided river systems

Scott R. Wilson[1], Jo Hoyle[2], Richard Measures[2], Antoine Di Ciacca[1], Leanne K. Morgan[3], Eddie W. Banks[4], Linda Robb[1], and Thomas Wöhling [1,5]

[1]Environmental Research, Lincoln Agritech, Lincoln University, New Zealand
[2]National Institute of Water & Atmospheric Research, Christchurch, New Zealand
[3]Waterways Centre for Freshwater Management, University of Canterbury, Christchurch, New Zealand
[4]National Centre for Groundwater Research & Training & College of Science & Engineering, Flinders University, Australia
[5]Chair of Hydrology, Technische Universität Dresden, Dresden, Germany

Correspondence to: Scott R. Wilson (scott.wilson@lincolnagritech.co.nz)

Abstract

Braided rivers can provide substantial recharge to regional aquifers, with flow exchange between surface water and groundwater occurring at a range of spatial and temporal scales. However, the difficulty of measuring and modelling these complex and dynamic river systems has hampered process understanding and the upscaling necessary to quantify these fluxes. This is due to an incomplete understanding of the hydrogeological structures which control river-groundwater exchange. In this paper we present a new conceptualisation of subsurface processes in braided rivers based on observations of the main losing reaches of three braided rivers in New Zealand.

The conceptual model is based on a range of data including lidar, bathymetry, coring, particle size distribution, groundwater, and temperature monitoring, radon-222, electrical resistivity tomography, and fibre optic cables. The combined results indicate that sediments within the recently active river braidplain are distinctive, with sediments that are poorly consolidated and better sorted compared to adjacent deposits from the historical braidplain which become successively consolidated and intermixed with flood silt deposits due to overbank flow.

29 A distinct sedimentary unconformity, combined with the presence of geomorphologically

30 distinct lateral boundaries, suggests that a "braidplain aquifer" forms within the active river

31 braidplain through the process of sediment mobilisation during flood events.

32 This braidplain aquifer concept introduces a shallow storage reservoir to the river system,

33 which is distinct from the regional aquifer system, and mediates the exchange of flow

34 between individual river channels and the regional aquifer. The implication of the new

35 concept is that surface water-groundwater exchange occurs at two spatial scales. The first is

36 hyporheic and parafluvial exchange between the river and braidplain aquifer. The second is

37 exchange between the braidplain aquifer and regional aquifer system. Exchange at both

38 scales is influenced by the state of hydraulic connection between the respective water

39 bodies. This conceptualisation acknowledges braided rivers as whole "river systems",

40 consisting of channels, and gravel aquifer reservoir.

41 This work has important implications for understanding how changes in river management

42 (e.g., surface water extraction, bank training and gravel extraction) and morphology may

43 impact groundwater recharge, and potentially on flow, temperature attenuation, and

44 ecological resilience during dry conditions.

46 **1.0 Introduction**

47 This study is motivated by the need to understand processes and quantify losses from

48 braided river systems to alluvial aquifers. In New Zealand more than 150 river systems are

49 thought to have braided reaches (Brower et al., 2024), which provide a substantial

50 component of recharge to alluvial aquifers. For example, in the case of the Wairau Aquifer,

51 it has been estimated recharge is sourced almost exclusively from the Wairau River

52 (Wöhling et al. 2018).

53   Braided rivers are spatially complex, dynamic hydrologic environments which are not easily

54   measured using field techniques or represented by numerical models. The determination of

55   flow exchanges between the river and groundwater in such a hydrologically complex and

56   morphologically dynamic environment is difficult because of their spatial and temporal flow

57   complexity, numerous and changing number of channels, dynamic bathymetry, coarse

58   substrate, and tendency for loss of field installations during high flow events. The

59   complexity of this challenge demands a collaborative effort that leverages the strengths of a

60   diverse range of disciplines to develop a comprehensive and holistic understanding of the

61   problem.

62   Many authors have studied surface-aquifer exchanges, and several reviews have been

63   conducted on available techniques for measuring exchanges for alluvial rivers in general

64   (Kalbus et al. 2006, González-Pinzón et al. 2015, Brunner et al. 2017), ephemeral rivers at

65   different spatial scales (Banks et al., 2011, Shanafield and Cook 2014), and braided rivers

66   (Coluccio and Morgan, 2019). Based on these reviews, there is a tendency for previous

67   studies to focus on quantifying exchange fluxes prior to understanding the hydrological

68   processes that influence the exchange. Ward and Packman (2019) suggest that despite the

69   large amount of research on river-groundwater exchanges, an accurate predictive,

70   transferable understanding of the river corridor is lacking. Indeed, a conceptualisation of

71   how braided rivers relate to their underlying groundwater systems is lacking (Coluccio and

72   Morgan, 2019). This has led to ambiguity in what measured exchanges represent, and

73   difficulty in trying to represent braided rivers within aquifer scale models.

74   The aim of this paper is to formulate a conceptualisation of braided river exchange

75   processes at both the local (reach) and sub-catchment (aquifer) scale. This conceptualisation

76   provides a framework for both providing context for field measurements of flow exchange

77   to be interpreted, and the potential for representation of local scale processes in sub-

78   catchment models. Incorporating these local scale processes is vital to predict how changes

79   in the river system can impact groundwater recharge.

80   The conceptualisation presented here was developed based on field observations but, for

81   clarity of explanation, we introduce the conceptual framework first and then present the

82   supporting evidence. Our working definition for hyporheic exchange is local bed-scale

83   interaction that occurs within a single channel (e.g., a single riffle), whereas parafluvial

84   exchange occurs between individual channels at larger scales (across a bar or further). We

85   also distinguish between a river as a series of wetted channels, and a "river system", which

86   consists of wetted channels plus subsurface flow through the associated braidplain gravels.

87   "Braidplain" refers to the lateral extent occupied by the river braids, old bar surfaces and

88   abandoned channels (Warburton, 1996; Gray et al., 2016; Brower et al., 2023). The extent of

89   wetted channels and recently reworked bed material (bare gravel) at a given point in time

90   defines the "active braidplain", which also has potential to shift laterally. Lateral adjustment

91   of the active braidplain may be limited by hillslope margins, terraces or, in managed rivers,

92   by rock revetments or artificial stop banks (levees) which are typically protected with

93   vegetative buffers. We refer to the extent within which our study rivers can currently adjust

94   as the "contemporary braidplain", acknowledging that in two of our study rivers (Wairau

95   and Ngaruroro) the contemporary braidplain margins are controlled by engineered flood

96   defences which have narrowed the natural braidplain such that almost the entire

97   contemporary braidplain is active.

98

99   **2.0 Review of existing concepts**

100   The prevailing conceptualisation for gravel bed rivers in general consists of a surface

101   channel with an associated bed with some hydraulic resistance (Schälchli 1992, Wu and

102   Huang 2000) which exchanges water with an associated fluvial or alluvial aquifer (Stanford

103   and Ward 1993, Poole and Berman 2001). Within the alluvial aquifer lies a hyporheic zone

104   which functions as an interface between groundwater and surface waters (Stanford and

105   Ward 1993, Poole and Berman 2001, Boano et al. 2014). The extent of the hyporheic zone is

106   defined by its function or process of interest, which can be physical, chemical, biological, or

107   a combination of functions (Ward 2015). Accordingly, the vertical or lateral boundaries of

108   the hyporheic zone are transient and flexible, and not easily defined spatially (White 1993,

109   Boulton et al. 1998, Ward 2015). From a hydrological perspective, the hyporheic zone has

110   been defined as the extent to which surface water enters the high porosity subsurface

111   beneath and lateral to a stream and returns to the stream surface farther downstream

112   (Harvey and Wagner, 2000). Authors have suggested the hyporheic zone as extending from

113   the upper few centimetres of sediment (Boulton et al. 1998, Sophocleous 2002) to larger

114   scales (km^3) constituting a hyporheic corridor (Stanford and Ward 1993). Valett at al. (1996)

115   predict the extent of the hyporheic zone to be related to catchment lithology, with

116   interaction being more extensive in sites with higher alluvial hydraulic conductivity, whereas

117   Boano et al. (2008) predict the infiltration depth to be related to bedform for any given

118   hydraulic conductivity.

119   An additional, ecological, concept is that of a riparian zone (Steiger et al. 2005). This extends

120   river margins beyond the active channel to include the biosphere supported by and

121   including recent fluvial landforms and inundated or saturated by bank discharge (Hupp and

122   Osterkamp 1996). Other authors have considered the presence of a parafluvial zone

123   situated between the hyporheic zone (beneath the river channel) and riparian zone (Holmes

124 et al. 1994) which accommodates longer flow paths within the alluvium adjacent to the

125 stream (Bourke et al. 2014, Cartwright and Hoffmann 2016). Our interpretation of the

126 parafluvial zone is that it constitutes exchange flow within the alluvial aquifer at spatial and

127 temporal scales beyond what is considered hyporheic.

128 From a hydrological perspective of braided rivers, the framework that emerges from the

129 prevailing concepts is one where river-groundwater exchange occurs within an alluvial

130 aquifer which conveys both hyporheic and parafluvial flowpaths. The proportion of these

131 flowpath components theoretically depends on the degree to which there is a net loss or

132 gain in river channel flow. However, the interpretation of river-groundwater exchanges

133 becomes challenging in a braided river which comprises multiple channels within an alluvial

134 aquifer. Harvey and Gooseff (2015), Barthel and Banzhaf (2016) and Ward and Packman

135 (2019) propose that exchange fluxes be considered at different spatial scales: point, local,

136 sub-catchment, and regional. Following this approach, exchange within individual river

137 braids or channels can be considered to occur at the point-scale, and the sum of all braids

138 within a river reach as a local-scale interaction. While process understanding can be

139 observed and fluxes quantified at the point and local scale, it is imperative to enable an

140 upscaling of observed processes so that fluxes can be estimated for at least the sub-

141 catchment (aquifer) scale.

142 Previous work on subsurface structure in braided rivers has tended to focus on the role of

143 bed material heterogeneity. A significant body of literature exists to describe braided river

144 deposits via morphology (Huber and Huggenberger 2016), sedimentology (Huggenberger

145 and Regli 2006, Theel et al. 2020), geophysics (Pirot et al. 2019), and modelling approaches

146 (Pirot et al. 2014; 2015, Brunner et al. 2017, Schilling et al. 2022). To date, no conceptual

147 model has been posed for how a braided river and its associated braidplain gravels (alluvial

148 aquifer) relate to those of the underlying regional aquifer. While the structural components

149 of river-groundwater interaction have been identified by previous authors (e.g. Poole and

150 Berman 2001, Steiger et al. 2005), the identification of clear spatial boundaries between

151 structural elements has been missing. From a hydrological perspective of understanding

152 surface water-groundwater interaction, this creates a problem of where the river system

153 ends, and where the regional groundwater system begins. The uncertainty related to this

154 lack of spatial definition transfers to the interpretation of field data, whether a sample is

155 representative of river channel flow, alluvial aquifer (hyporheic or parafluvial zones), or

156 regional groundwater.

157 Consequently, representation of braided rivers in numerical models is problematic since

158 their complexity is not readily captured by a simple conceptualisation. Water exchanges can

159 potentially be simulated realistically using a fully coupled hydrological model such as

160 HydroGeoSphere (Therrien et al. 2010, Brunner and Simmons 2012). However, the data

161 required to parametrise such a model, and the computational demands of the detailed

162 mesh required to simulate exchanges in braided rivers make this approach only suitable for

163 point and local scale studies. Furthermore, braided river morphology is so dynamic that a

164 new bed morphology would be required following each significant flood event. In recent

165 years, two approaches to simulate the transitions of dynamic bed morphology and

166 sediments on river-groundwater exchanges have been tested. The first approach applied

167 the ensemble Kalman filter and areal imagery to assimilate river bed topography and to

168 update aquifer hydraulic conductivities in a HydroGeoSphere model for a 2-km section of

169 the Emme River in Switzerland (Tang et al. 2018). The data assimilation scheme strongly

170 improved predictions of post-flood hydraulic states of the system. The second approach

171 proposed a pilot point parametrization scheme where both the aquifer properties (hydraulic

The simple river structure offered by the Streamflow-Routing (SFR, Niswonger and Prudic, 2005) and River (Harbaugh, 2005) packages in MODFLOW represent the river as a flux boundary condition with vertical flow impedance in the bed expressed by a lumped parameter termed 'streambed conductance'. Previous authors have shown that the concept of a streambed resistance concentrating all pressure losses, as implemented in MODFLOW, is questionable in many cases (Anderson 2005, Rushton 2007, Morel-Seytoux et al. 2018, Di Ciacca et al. 2019). Moreover, even if such a streambed exists, a major physical issue with a lumped parameter approach is that streambed conductance values in the field are not homogenous, but vary spatially (Cardenas and Zlotnik 2003, Zhou et al. 2014, Pryshlak et al. 2015, Laube et al. 2018) and temporally (Levy et al., 2011, Wu et al. 2015). In a braided river, bed material typically consists of a heterogeneous mixture of cobbles, gravels, and sands, which can have similar characteristics to alluvial sediments located several metres beneath the bed. Therefore, the streambed conductance concept seems inappropriate to represent surface water-groundwater exchange in braided river systems.

Different modelling approaches have been trialled to represent braided rivers in New Zealand. White et al. (2012) conducted a steady state water balance approach to determine flow losses for a reach of the Waimakariri River. Exchanges between individual channels and the adjacent alluvial aquifer were determined via mass balance, although the subsurface

196   components of the exchange were not explicitly described. An alternative approach by

197   Wöhling et al. (2018, 2020) simulated dynamic Wairau River exchanges at the sub-

198   catchment scale using MODFLOW. In this case, the braided nature of the river was not

199   considered, and the river was represented by the SFR package using a stage-width-flow

200   relationship derived from a representative channel morphology. While this model fitted

201   river flux and groundwater level data well, the approach employed a streambed

202   conductance model, which is difficult to reconcile with the river morphology and bed

203   sediment seen in the field. A particular drawback of the SFR package is its inability to

204   represent the hyporheic or parafluvial exchange fluxes observed at the point or local scale.

205   While the Waimakariri and Wairau modelling studies are relatively comprehensive, in both

206   cases, an understanding of subsurface structure is missing from the river representation.

207   This lack of knowledge about the structural controls on subsurface flow in the braided river

208   environment needs clarification to understand what measured and modelled river-

209   groundwater exchanges represent. In doing this, a more physically realistic method for

210   representing braided rivers in numerical surface water-groundwater flow models may be

211   achieved.

212

213   **3.0 Proposed conceptualisation**

214   A conceptual framework is proposed which captures the key elements of water exchanges

215   in a braided river system. This conceptualisation builds on the previous work of Fox and

216   Durnford (2003) and Brunner et al. (2009a and b) and recognises that the hydrological

217   controls on river-groundwater exchange occur at two distinct interfaces within a braidplain

218   system. Specifically, these two exchange processes can be summarised as:

219   1.   River channel ↔ braidplain aquifer (hyporheic and/or parafluvial exchange)

220	2. Braidplain aquifer ↔ regional aquifer ("river system" - groundwater exchange)

221	The first exchange interface is within the active braidplain, and occurs between individual

222	river channels (braids) and the local shallow water-table in the river bed sediments, and

223	occurs at the point or local scale. We term the water stored within these river bed

224	sediments the "braidplain aquifer" (BPA), which facilitates hyporheic and parafluvial flow.

225	For a perennially flowing river, the BPA will retain some degree of saturation throughout the

226	year, although unsaturated conditions may occur in the case of intermittent or ephemeral

227	rivers if there are prolonged periods with no river flow. Individual river braids can be in

228	hydraulic connection (gaining or losing), disconnection, or a transitional state relative to the

229	BPA. At the active braidplain interface, all possible river exchange processes can occur

230	regardless of the hydraulic relationship between the BPA and surrounding regional water

231	table. The second exchange interface occurs at both the local (reach) and sub-catchment

232	(aquifer) scale, between the BPA and regional water table.

233	Central to this conceptualisation is the presence of a distinct BPA immediately beneath the

234	river surface which facilitates exchange at these two interfaces. A similar term "braided-

235	river aquifer" has been used by previous authors (Pirot et al. 2015), although we have not

236	found an associated definition. The BPA functions as a storage medium to exchange water

237	between the river and regional aquifer in braided river systems. Direct exchange of water

238	between the river and regional aquifer can only occur if the river channel is in direct contact

239	with the regional aquifer (i.e., where the surface water extends to the boundary of the BPA,

240	for example where a channel follows the lateral margin of the BPA, or there is a connection

241	at the base of a deep scour pool).

242	A key feature of the BPA is its extremely high transmissivity, which is a product of the highly

243	dynamic nature of braided rivers. Bedload transport during flood events causes braids to

244 form, migrate, and be abandoned; processes that re-work the river bed sediments (Bristow

245 and Best, 1993; Reinfelds and Nanson, 1993). This reworking process strips most fine

246 sediment (silts and clays) from the river bed, as the shear stresses during floods are too high

247 for these size fractions to be deposited except in vegetated areas and backwaters. The

248 result is a braidplain deposit of high transmissivity lag gravels. High transmissivity combined

249 with the relatively large bed slope of braided rivers and the presence of multiple braids for

250 water exchange produces a groundwater flow path which is sub-parallel to the

251 contemporary braidplain, regardless of the regional groundwater flow direction.

252 Conceptual diagrams have been drawn for situations where the BPA is hydraulically

253 disconnected from (Figure 1a) and connected to (Figure 1b) the regional aquifer. The first

254 case (Figure 1a) consists of three functional lithological layers representing a BPA which is

255 hydraulically disconnected from an underlying regional aquifer by an unsaturated zone. In

256 this case, water moves vertically from the BPA to the regional aquifer under a unit hydraulic

257 gradient. A minimum of three layers is required for an unsaturated zone to develop (Fox and

258 Durnford, 2003), and there must be a sufficient transmissivity contrast between the

259 impeding horizon and underlying sediments (Brunner et al., 2009a and b). It should be

260 noted that braided river deposits are lithologically variable and complex, and in most cases

261 only two functional layers are required due to stratification in the underlying sediments.
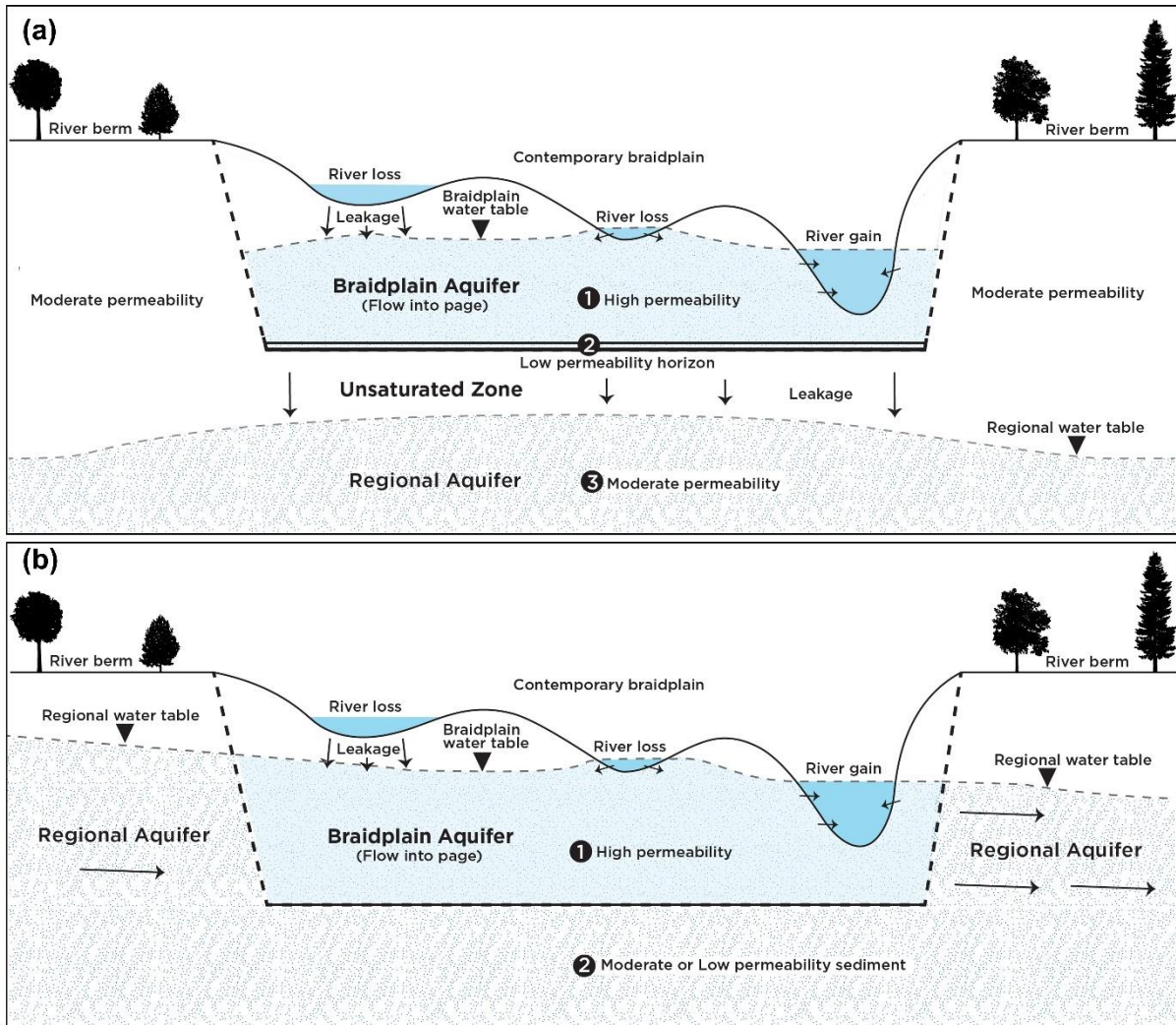
Figure 1. Conceptualisation for a braidplain aquifer which is (a) hydraulically disconnected

from or transitional with the regional groundwater system, and (b) hydraulically connected

to the regional groundwater system.

A hydraulically disconnected river system setting shares features in common with

intermittent or ephemeral rivers (Shanafield et al. 2021). Infiltration to the regional aquifer

is regulated by the vertical resistance of lower permeability sediments and the hydraulic

head in the BPA. If the BPA is fully saturated across the contemporary braidplain, the rate of

infiltration to the regional aquifer will be steady because the braidplain has reached a

maximum wetted area. In this condition, some minor temporal infiltration variability will

273   occur due to changing water levels in the BPA. Under ephemeral conditions, the saturated

274   extent of the BPA decreases longitudinally, and locally laterally, during drying phases in

275   response to extended periods of low river flow. The combined reduction in head and

276   saturated area of wetted braidplain result in considerably less infiltration to the regional

277   aquifer (Di Ciacca et al. 2023).

278   The second case is a setting where the river is hydraulically connected to the regional

279   aquifer system (Figure 1b). A minimum of two lithological units are present, a high

280   transmissivity BPA and regional aquifer (1) overlying less permeable sediments (2) which

281   impede vertical flow. The combination of these two factors creates an anisotropy, with

282   preferential flow in the lateral direction. Hydraulically gaining conditions will occur in

283   situations where regional water levels are elevated by low permeability boundaries (i.e. the

284   presence of bedrock) on one or both sides of the river, or at middle to distal positions on

285   alluvial fans where regional groundwater levels are closer to the land surface.

286   For a hydraulically connected river system (braids + BPA), the hydraulic gradient is no longer

287   vertical, as it is for the hydraulically disconnected scenario, but variable, with the exchange

288   rate governed by the relative hydraulic gradient between the braidplain and regional

289   aquifers. Thus, groundwater inflow to the BPA or discharge to the regional aquifer can occur

290   laterally along both margins of the braidplain, as well as vertically through BPA base. The

291   setting can also be asymmetric, with inflow on one margin, and outflow on the other (as

292   shown in Figure 1b), with the total river system water balance being gaining or losing, or

293   having no flow along one margin due to the presence of bedrock.

294   While the hydraulically connected situation is simpler structurally, relative to the

295   disconnected situation, exchange between the braidplain and regional aquifers is more

296   complex. In this case (Figure 1b), water exchange is governed by the hydraulic gradient

297 between the two aquifers, the transmissivity of both aquifers, and the vertical hydraulic

298 conductivity of the underlying sediments. Once water exits the BPA in a losing reach, it will

299 not return unless it is re-routed back to the river system by a reversal of the hydraulic

300 gradient.

301 The sedimentological features and groundwater-surface water interaction concepts

302 associated within the contemporary braidplain have been identified and detailed by

303 previous authors (e.g., Huggenberger et al. 1998). Regardless of the nature of the

304 relationship between the braidplain and regional aquifers, the braidplain gravels have a

305 higher transmissivity than both the adjacent and underlying sediments because of repeated

306 reworking of the braidplain gravels during high flow events. Hyporheic and parafluvial flow

307 occurs within these highly transmissive BPA sediments, subparallel to the river flow

308 direction, with individual braids acting as recharge or discharge boundaries. As such, the

309 local hydraulic gradient and groundwater flux are largely influenced by river bathymetry.

310

311 **4.0 Locations and methods for concept validation**

312 *4.1 Catchment descriptions*

313 The conceptualisation presented here is based on field observations of the main losing

314 reaches of three braided rivers in the drier eastern part of New Zealand (Figure 2). These

315 are, from north to south, the Ngaruroro (a), Wairau (b), and the Waikirikiri (c, also known as

316 the Selwyn). These study areas were selected to take advantage of the potential for

317 hydrological separation afforded by dominantly losing river reaches. The downward

318 hydraulic gradient, and potential hydrological separation between channel, bed gravels and

319 regional aquifer enable the possibility for different structural and hydrological components

320   to be identified. Summary hydrological and geomorphological statistics for the three study

321   sites and their source catchments are shown in Table 1.

322
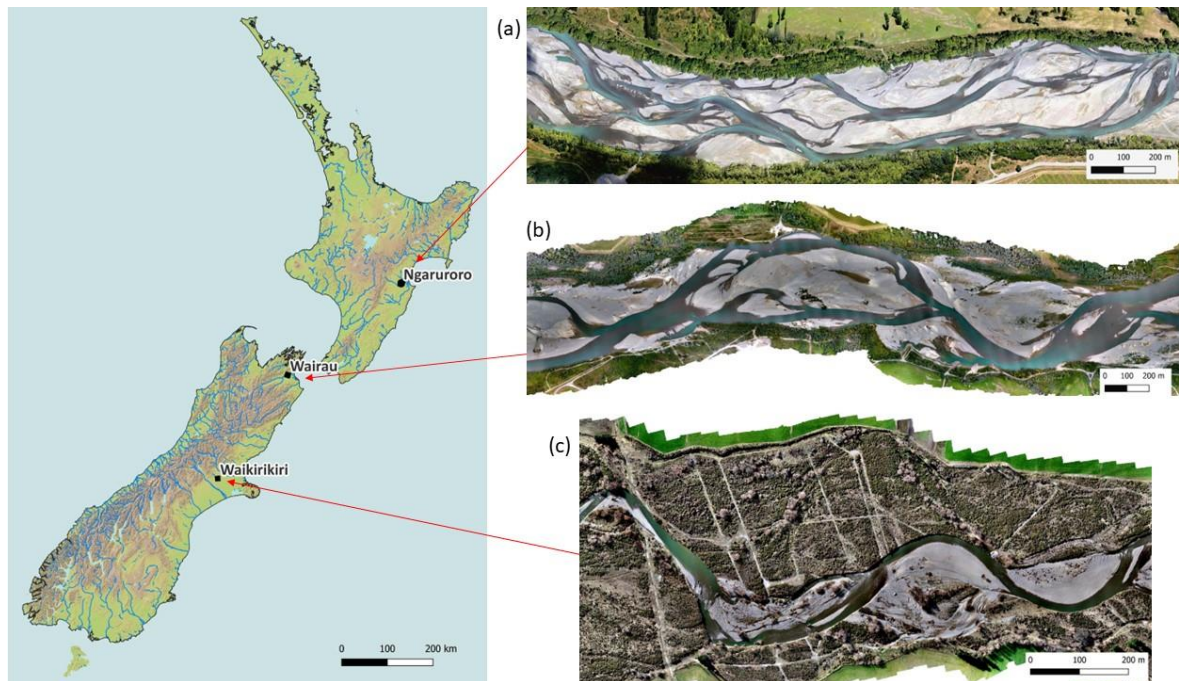
323

324   **Figure 2**. Location of the three study rivers and their aerial images

325

326   The Ngaruroro River is 164 km long, and has its headwaters in the Kaweka, Kaimanawa, and

327   Ruahine ranges on the main divide of the North Island. The 3 km long study reach is located

328   at the margin of the Heretaunga plain between Roy's Hill and Fernhill and is the main

329   recharge source for the Heretaunga alluvial aquifer system (Dravid and Brown, 1997). A

330   long-term flow monitoring site at Fernhill (70 years), situated at the lower end of our study

331   reach, has recorded a mean flow of 40 $m^3.s^{-1}$ and mean annual peak flow of 1546 $m^3.s^{-1}$. The

332   Ngaruroro study reach is in a natural depositional zone within the catchment (i.e., bedload

333   into the reach exceeds that leaving the reach). This reach typically has 3 braids, with the

334   active braidplain confined between willow plantings.

335

336 The Wairau River (Wöhling et al., 2018 and 2020) is 170 km long, and has its headwaters in

337 the alpine Spencer Range on the main divide of the South Island. As such, the Wairau

338 receives considerable source water from rain at higher elevations, producing a mean flow of

339 100 $m^3.s^{-1}$, and high mean annual peak flow of 1911 $m^3.s^{-1}$ (63 years of record at SH1). The

340 Wairau River is also "flashy", with over ten events exceeding three times the median flow

341 annually (FRE3, Booker 2013). The 2.2 km long study reach is in the middle section of the

342 Wairau Plain, between Jeffries and Giffords roads. This study reach typically has 2 braids and

343 the active braidplain is confined between engineered rock revetments and groynes. Bedload

344 flux into and out of this reach is approximately equal (bedload transfer zone).

345 The Waikirikiri River has its headwaters in the foothills of the Southern alps and receives

346 considerably less runoff than the other rivers. The 1 km long study reach is situated near

347 Hororata where the river leaves the foothills and crosses the western margin of the

348 Canterbury Plain. A long-term (58 years) flow monitoring site located upstream of the study

349 reach at Whitecliffs shows a mean annual flow of 4.5 $m^3.s^{-1}$, and peak annual flow of 28

350 $m^3.s^{-1}$. The Waikirikiri River is also the least "flashy" with an average of only one event each

351 year exceeding a flow of three times the median flow. As a result of its lower flow and high

352 transmission losses, the Waikirikiri River is subject to intermittent flow within our study

353 reach (Larned et al., 2008; Di Ciacca et al., 2023). The Waikirikiri study reach is naturally

354 incised between Pleistocene terraces, with no engineered flood controls. The active

355 braidplain, which typically has 1-2 braids, can freely adjust between these contemporary

356 braidplain margins, however, relatively dense exotic vegetation covers much of the

357 contemporary braidplain.

358

359   **Table 1.** Characteristics of the three study catchments. Mean values are given unless stated

360   otherwise. FRE3 is the annual number of events exceeding three times the median flow. Bed

361   material grain size is near surface but excludes the armour.

	Ngaruroro	Wairau	Waikirikiri
Study reach length (m)	3000	2200	1000
Contemporary braidplain width in study reach (m)	300	400	460
Active braidplain width in study reach (m)	300	400	55
Braiding index in study reach	2.95	1.96	1.56
Reach slope (m.m^{-1})	0.003	0.003	0.006
Catchment Area (km^2)	1930	3320	250
Catchment rainfall (mm.y^{-1})	1414	1543	1045
Catchment potential evapotranspiration (mm.y^{-1})	722	693	750
Annual low flow (m^3.s^{-1})	1.2	9.9	0.97
Median flow (m^3.s^{-1})	23.1	61	2.35
Mean flow (m^3.s^{-1})	40	100	4.5
Annual peak flow (m^3.s^{-1})	1546	1911	28.3
FRE3	6.1	10.7	1.1
River loss at study reach (m^3.s^{-1}.km^{-1})	~0.6	≥0.2	0.25-0.65

362

363   All three rivers share a similar bedload lithology dominated by Jurassic greywacke. In the

364   study reaches, the Ngaruroro is bounded to the north by Pliocene siltstone and limestone

365   (Lee et al. 2011), while the Wairau is bounded to the north by schist (Begg and Johnston

366   2000). These two rivers lose water southwards, the river losing reaches being the primary

367   source of recharge for the alluvial aquifers hosted by Holocene gravels. In the Waikirikiri

368   study reach, the river is bounded by Pleistocene glacial outwash gravels (Forsyth et al.

369   2008). These gravels form the surface expression of a large, stratified aquifer system hosted

370   by a composite of alluvial fans which underlies the Canterbury Plains. The Ngaruroro and

371   Waikirikiri study reaches are both situated close to the apex of the river system's alluvial fan

372   (close to where the rivers emerge from the foothills).

373

374   Both the Wairau and Ngaruroro are affected by gravel extraction, which has lowered the

375   mean active braidplain bed elevation in the river recharge reaches by approximately one

376   metre since the 1980's (Gardner and Sharma 2016, Measures 2012). The varying physical

377   environments, flow regimes, bed adjustment trajectories, and degree of lateral confinement

378   result in different rates of bed reworking for each river. In particular, the Waikirikiri reworks

379   its bed less frequently than the Ngaruroro and Wairau.

380

381   *4.2 Field data collection*

382   Investigations in the study reaches involved the collection of a variety of data types (Table

383   2). Each method and data type has advantages and disadvantages and is scale and process

384   dependant (Gonzalez-Pinzon et al., 2015; Brunner et al., 2017). Stage and temperature

385   recorders were established in the study reaches but were difficult to maintain due to

386   repeated destruction by flood flows and frequent bed movement in the study reaches. Flow

387   rating was conducted at the top of the reach for the Waikirikiri River, and permanent rated

388   flow sites located downstream were used for the Ngaruroro and Wairau. A series of flow

389   loss gauging surveys were undertaken at multiple transects within all three study reaches

390   across a range of discharges to estimate transmission losses. Due to the difficulty of

391   measuring flow in the larger rivers (and the related large measurement uncertainty), the

392   most comprehensive set of flow loss surveys was conducted on the Waikirikiri (Di Ciacca et

393   al., 2023).

394

395   Table 2. Type and number of measurements undertaken in the three study reaches.

Measurement type	Ngaruroro	Wairau	Waikirikiri

Differential flow gauging	2	2	14
Local river stage/temperature		3	6
LiDAR and bathy surveys	1	2	2
Piezometers	19	31	43
Cored holes	10	8	21
Particle size distribution	36	38	60
Core porosity	6	12	5
Field porosity	3	10	4
Radon-222 samples	5	53	61
tTEM	Y	Y	Y
DualEM	Y	Y	Y
SkyTEM	Y		
ERT surveys		9	11
Ground penetrating radar (GPR)			5
DTS installations (vertical)		2	3
DTS installations (horizontal)			2

396

397 LiDAR data were captured in dry areas of riverbed using a LiDARUSA Snoopy LiDAR scanner

398 deployed on either a UAV or backpack. Bathymetry and water surface elevation were

399 mapped using a kayak or remote controlled jetboat equipped with a paired RTK GPS and

400 echosounder, and wading with an RTK GPS. Interpolation, or (where necessary) optical-

401 bathymetry techniques, were used generate high-resolution bathymetry maps from less-

402 dense echosounder survey data. The dry topography from LiDAR was stitched together with

403 the bathymetry data to provide a complete digital elevation model (DEM) for each reach at

404 a spatial resolution of 1 m or less, and a vertical accuracy of ±0.1 m in dry areas and ±0.2 m

405 in wet areas.

406 Piezometers were installed at different depths to provide a time series of water levels and

407 temperature, and to enable sampling for radon-222 analysis. The piezometers were

408 installed with 50mm diameter PVC. Screens were a 1-2m length of slotted casing with a

409 geotextile sock and sand pack around the screen, and cement grout around the overlying

410 casing. A sump was used to collect downward percolating water in situations where pore

411 water pressure was below saturation. Drilling methods involved a mix of rotary and sonic

412   drilling, the former being used to install the piezometer network. Sonic drilling with a

413   Geoprobe 8140LC (76.2mm diameter core) was conducted to collect cores for detailed

414   logging and sediment analysis (grainsize and porosity). The sonic drilling method is not ideal

415   as it can be difficult to get good core recovery, particularly in coarser or loose near-surface

416   sediments. As a result, the core record is incomplete, however, there is currently no better

417   method available to extract several meters of core from coarse riverbed deposits. Because

418   core recovery was variable, data from individual drillholes were fragmented, and sediment

419   analysis was only conducted on the most intact cores (0.1-1.2 m in length), with samples

420   taken for grainsize and porosity analysis. Near-surface bed material grain size distribution

421   and porosity were measured using manual excavation sieving combined with a detailed

422   photogrammetry method to calculate excavation volume (Montgomery et al. subm.).

423   Particle size distribution was characterised by fitting Gompertz and Weibull curves (Bayat et

424   al. 2015) to the sieved sediment data, and summary statistics determined via the method of

425   Folk and Ward (1957).

426   The base of the BPA was identified in two ways. The first method was by mapping surface

427   morphology, since the deepest areas of pools represent the scouring depth that has

428   occurred during flooding. Surface and bed morphology was captured using remote sensing

429   (photogrammetry, LiDAR, and bathymetry). The second method was through observations

430   in drill core with good core recovery, where sediments beneath the BPA are characterised

431   by more cohesion and a finer matrix. To enable data to be compared, contacts between the

432   braidplain gravels and underlying sediments (depositional unconformity) have been

433   expressed as depth below a detrended surface representing cross-section mean

434   contemporary braidplain surface elevation. This datum was chosen because of the spatially

435   variable and temporally dynamic river bed levels.

436 Hydrogeophysical methods were also used to image the subsurface, including passive (DTS)

437 and active (ADTS) distributed temperature sensing (Banks et al., 2022), ground penetrating

438 radar (GPR), electrical resistivity tomography (ERT), transient electromagnetic (tTEM) and

439 electromagnetic induction (DualEM421). The tracks prepared for tTEM and DualEM surveys

440 are evident in the aerial photos shown in Figure 3. SkyTEM data were also available for the

441 Ngaruroro area (Rawlinson et al. 2021). Of the hydrogeophysical methods employed,

442 DTS/ADTS, and ERT were the most successful methods for delineating sediment structure

443 and saturation associated with the river. The resistivity of New Zealand braided river water

444 (fluid specific conductance ~5 mS.m^{-1}) and associated gravel deposits is very high (400-

445 10,000 Ωm). For this reason, we think there was insufficient resistivity contrast for

446 electromagnetic and ERT methods to reveal distinct subsurface features in most of our

447 surveys. SkyTEM data did provide good definition of the basement contact beneath the

448 Ngaruroro River but did not reveal any clear structural features in the near surface (<10 m).

449 GPR surveys that were trialled at the Waikirikiri site clearly revealed the shallow water table

450 but did not reveal any clear structure beneath the water table due to reflection of the

451 signal.

452 Samples for radon-222 analysis were collected in 250 ml bottles in the Waikirikiri (Songola

453 2022) and Wairau reaches from riffles, at different depths in pools, and from purged

454 piezometers. Samples were analysed 21-100 hours after sampling for Waikirikiri, and 20-24

455 hours for the Wairau. Laboratory analysis for radon activity was conducted with a RAD7

456 (Durridge 2020a), RAD H2O (Durridge 2020b), and active DRYSTIK (Durridge 2021) in a

457 closed loop system, with the results adjusted for decay since the time of sampling (WAT250

458 method). The radon activity and uncertainty values reported here follow the approach of

459 Durejka et al. (2019), with the mean and standard deviation calculated from five counting

460 cycles, with duplicate samples pooled (ten cycles total). Additional radon measurements

461 were made in the field using the RAD AQUA method (Durridge 2020c) to verify the WAT250

462 method results, and these returned similar values. For this study we have reported the

463 WAT250 data, which has a larger uncertainty associated with the measurements but

464 enables more samples to be collected in a short time frame from remote field sites. To

465 reduce the uncertainty of the WAT250 results, we increased the aeration time to 10

466 minutes, and the analysis duration recommended in the Durridge manual to 5 cycles of 10

467 minutes.

468

469 **5.0 Field observations**

470 A hydraulically disconnected river-regional aquifer system has been identified from drilling

471 and monitoring data in the Waikirikiri study reach (Banks et al. 2022, Di Ciacca et al. 2023),

472 and at the upper part of the Ngaruroro study reach. A hydraulically connected river-regional

473 aquifer system is observed in the Wairau study reach, and in the lower part of the

474 Ngaruroro study reach. Evidence for the proposed conceptualisation is provided below

475 based on data type. Data referred to in the text and figures is shown spatially in Figure 3.

476 Points where the base of the BPA has been observed in cores, or inferred via deep pools are

477 identified.

478
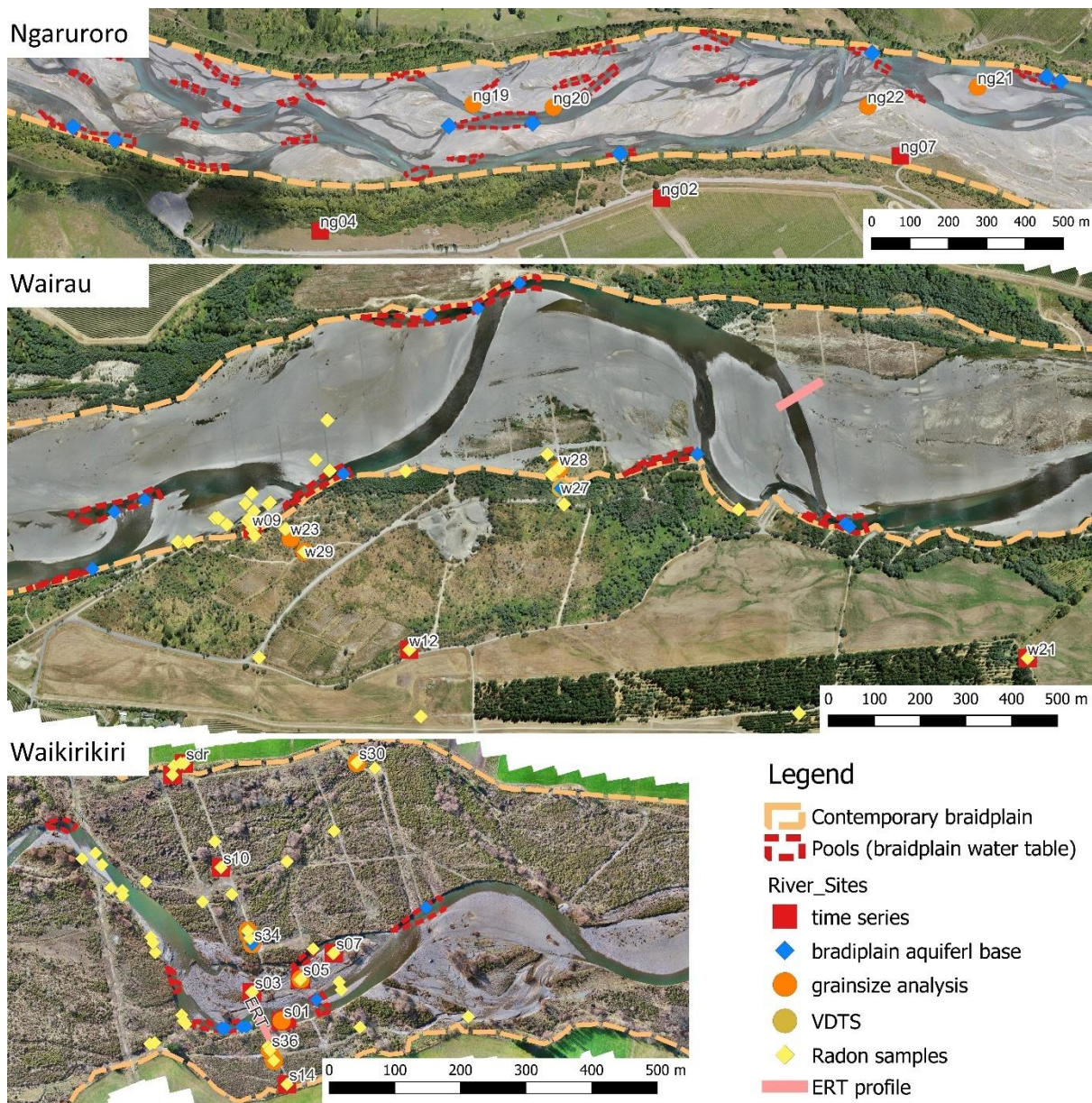
Figure 3. Data sources referred to in the text.

5.1 Geology and geomorphology

The BPA lateral extent in our three sites is identified geomorphologically as being at the

contemporary braidplain margins (orange dashed lines in Figure 3). The contemporary

braidplain margins in our study reaches are either artificially confined by rock armouring or

willow planting for flood protection (Wairau and Ngaruroro), or by terrace boundaries

(Waikirikiri). These relatively static lateral controls result in the abutment of relatively loose

488   (recently active) braidplain gravels against older, more poorly sorted sediments. In the

489   Wairau and Ngaruroro rivers the artificial lateral controls are sufficiently narrow that the

490   entire contemporary braidplain is regularly reworked (i.e., the active braidplain margins and

491   contemporary braidplain margins are essentially the same). In the Waikirikiri, the active

492   braidplain is narrower than the contemporary braidplain and the active braidplain is able to

493   adjust laterally, reworking the contemporary braidplain gravels.

494   In all three braided rivers, deep pools form at the toe of riffles. In the Wairau and

495   Ngaruroro, these are amplified at the braidplain margins where river flow is reflected by

496   rock armouring or willow plantings that limit lateral erosion and enhance bed scour. These

497   pools are zones where the BPA discharges to the river. Parafluvial seeps are commonly

498   observed in these locations, which have higher radon-222 activities and summer

499   temperatures that are cooler than adjacent river braids. The surface expression of the BPA

500   can be seen in abandoned channels where the braidplain surface topography drops below

501   the braidplain water table and exposes groundwater (static pools or flowing springs). These

502   areas are demarked by dashed red lines in Figure 3.

503   The depositional unconformity at the BPA base in recovered cores was observed at 1.7-2.0

504   m depth beneath the mean bed level of the contemporary braidplain in the Ngaruroro study

505   reach, 4.3-5.0 m depth in the Wairau, and 2.1-3.7 m depth in the Waikirikiri. The greater

506   depth in the Wairau River is unsurprising, as this river has the highest flood flows and is

507   tightly confined by engineering works, resulting in greater depths of bed reworking.

508   At the Waikirikiri site, the contact of the depositional unconformity was seen as a change

509   from grey-brown postglacial sandy gravels to yellow-brown clay-rich glacial outwash gravels

510   (Figure 4). During drilling and completion of the groundwater monitoring wells, a drop in the

511   water level with depth below the glacial contact was observed. Six cores were drilled just

512   beneath the unconformity at various locations within the contemporary braidplain margins

513   to investigate the saturation status beneath the braidplain gravels. These holes were drilled

514   through the low permeability contact layer until an apparent increase in permeability was

515   encountered, at which point the water level in the drillhole dropped significantly.

516   Piezometers screened beneath the base of the BPA and above the regional water table

517   showed low and unvarying water levels, indicating unsaturated or variably saturated

518   conditions (Figure 7). Our explanation for the presence of this variably saturated zone is that

519   the glacial outwash gravels are stratified, and vertical infiltration to the regional aquifer is

520   limited by the lower permeability horizons of silt and clay. The presence of higher

521   permeability horizons within the stratified postglacial sequence allows water to move

522   laterally away from the recharge zone at a rate that exceeds vertical infiltration, enabling

523   unsaturated or variably saturated conditions to form.

524
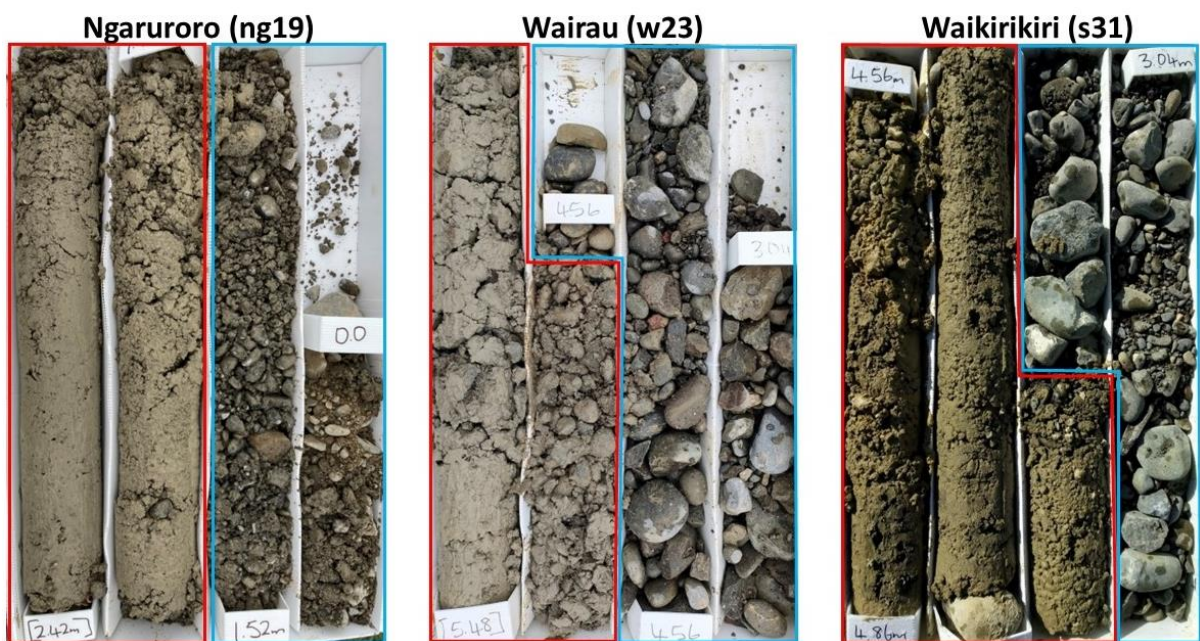
526   **Figure 4.** Representative core samples across the unconformity at the three study sites

527   (blue=braidplain gravels, red=underlying very poorly sorted consolidated gravels)

528

At the Wairau River study site, the base of the BPA is visible as a change from grey-brown

sandy clast supported gravel to more cohesive and poorly sorted gravel with increasing

proportions of silt and clay. Just beneath this unconformity is a more prominent contact

with yellow brown silty clay-bound gravel associated with old outwash fan deposits along

the Richmond Range (not shown in Figure 4, but evident in Figure 10). Note that some of

the Wairau core holes were positioned on the berms (outside of what we are referring to as

the contemporary braidplain), where the active braidplain was located prior to river re-

alignment in the 1960s. The river can no longer mobilise sediments on these berms due to

rock armouring of the banks leaving a recent remnant braidplain gravel deposit beneath the

southern berm. This deposit is both spatially and vertically separate from the contemporary

braidplain (the mean bed level of the contemporary braidplain is approximately 2m below

the berms).

In the Ngaruroro study site, the unconformity at base of the BPA is more gradational,

manifesting as an increase in silt and clay content between 1.7 and 2.0 m depth visible

within bore logs (Figure 4) and particle size distribution (Figure 5). As with the Waikirikiri

River, a drop in the water table was observed while drilling beneath this lower permeability

unconformity. The less-distinct base to the BPA in the Ngaruroro study reach is likely

because the reach is depositional, so the underlying gravels were deposited relatively

recently compared to the other study reaches.

Particle size distribution summary statistics of core samples collected by sonic drilling and

bed excavation are shown in Figure 5, with classifications according to the Folk and Ward

(1957) scale. A relationship between sorting and grainsize is apparent at each site, with

poorer sorting corresponding to an increase in the finer fraction. Shallow braidplain gravels

552   are overall poorly sorted (1-2, data mean: Ngaruroro 1.98, Wairau 1.90, Waikirikiri 1.96),

553   whereas the underlying gravels tend to be very poorly sorted (2-4, data mean: Ngaruroro

554   2.88, Wairau 2.28, Waikirikiri 2.60). The grainsize of the braidplain gravels is generally

555   coarser (mean: Ngaruroro -4.76, Wairau -4.23, Waikirikiri -3.55) than the underlying very

556   poorly sorted sediments (mean: Ngaruroro -1.64, Wairau -3.54, Waikirikiri -2.69).

557
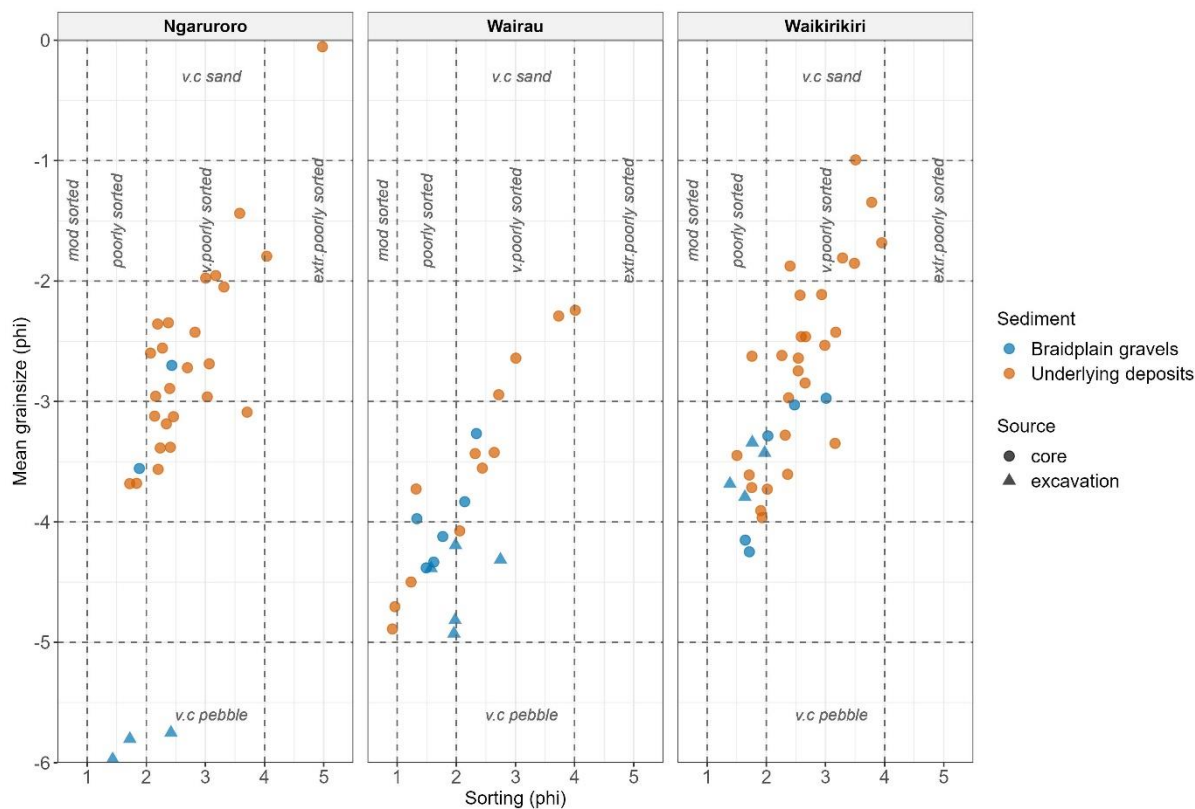
558

559   **Figure 5.** Grainsize analyses and sorting indices from samples beneath the three study

560   reaches. Dashed lines are breaks for grainsize and sorting indices (after Folk and Ward

561   1957).

562   Core recovery at all sites was typically poor in the contemporary braidplain gravels, which

563   mostly consist of loose gravel and cobbles, with a high proportion of sand but only a trace of

564   silt and clay. Because of this, some of the braidplain gravel samples have been sourced from

565   samples manually excavated from the braidplain subsurface (Figure 5). These excavated

566   samples exclude the surface armour common in gravel bed rivers. For the Wairau data set

567   there is no clear separation in the particle size distribution between braidplain and

568   underlying gravels. Wairau sediments are coarser than the other two sites, because of the

569   high-energy of this river system. The coarseness of the sediments greatly hampers core

570   recovery, so it is possible that the lack of separation is an artefact of the loss of finer

571   fractions in some samples during drilling.

572

573   *5.2 LiDAR and bathymetry*

574   LiDAR and bathymetry surveys were conducted in each study area to understand the

575   spatially varying relationship between the river surface, bed levels, and water levels in the

576   braidplain and regional aquifers. Repeat surveys were conducted following significant flood

577   events to capture changes in bed levels. An example of our LiDAR and bed elevation data for

578   the Wairau River is shown in Figure 6. These data were captured on 19 Feb 2020 at

579   relatively low flow conditions, measured at 13.4 $m^3.s^{-1}$ to 11.5 $m^3.s^{-1}$ (±3 %) at the upstream

580   (left) and downstream (right) margins of Figure 6 respectively. The river water surface and

581   bed elevation data within the wetted channel are shown on Figure 6 in relation to a

582   modelled surface of hydraulic head across the river system, represented by piezometric

583   contours which are shown in Figure 6a. This surface was fitted (sum squared error of 5 x 10$^-$

584   ^{6}) to 25 water level observations (yellow points in Fig 6a) located within and outside of the

585   contemporary braidplain by universal kriging with an exponential variogram of anisotropy of

586   0.9 at 090°, partial sill 0.31 m, and range 670 m. With such a large variogram range, the

587   surface should be considered as indicative of an averaged hydraulic head across the regional

588   and braidplain aquifers. The kriged surface does reveal an inflection of the piezometric

589   contours across the contemporary braidplain margins, indicating that flow within the BPA is

590   largely controlled by river exchange and preferential flow within the BPA, with flow being

591   approximately sub-parallel to the contemporary braidplain longitudinal orientation.

592   Fig. 6a reveals locations in the river system where the river water surface is higher than the

593   braidplain water table (red and orange zones), indicating that the river is losing flow to the

594   BPA in these areas. Areas of the river which are coloured blue in Fig. 6a represent the

595   surface expression of the braidplain water table in pools. These are locations where the

596   river can potentially gain flow. The black areas denoted as "riffles" are identified from a

597   slope raster derived from the digital elevation model (DEM). Locations where maximum

598   potential river water loss occurs can be identified in most cases as being situated at the

599   upstream margins of high elevation riffles.

600   The bathymetry DEM (Fig. 6b) reveals the presence of scouring along the contemporary

601   braidplain margins, which in the case of the Wairau River is promoted by excessive river

602   narrowing and rock training banks. The corollary of this scouring is the relative mounding of

603   gravel in the middle of the contemporary braidplain. The difference between the river bed

604   level and hydraulic head reveals locations where the river bed is above the braidplain

605   aquifer, and the river braid has the potential to be losing-disconnected at these locations. In

606   most cases these areas also correspond to the upstream margins of high elevation riffles.
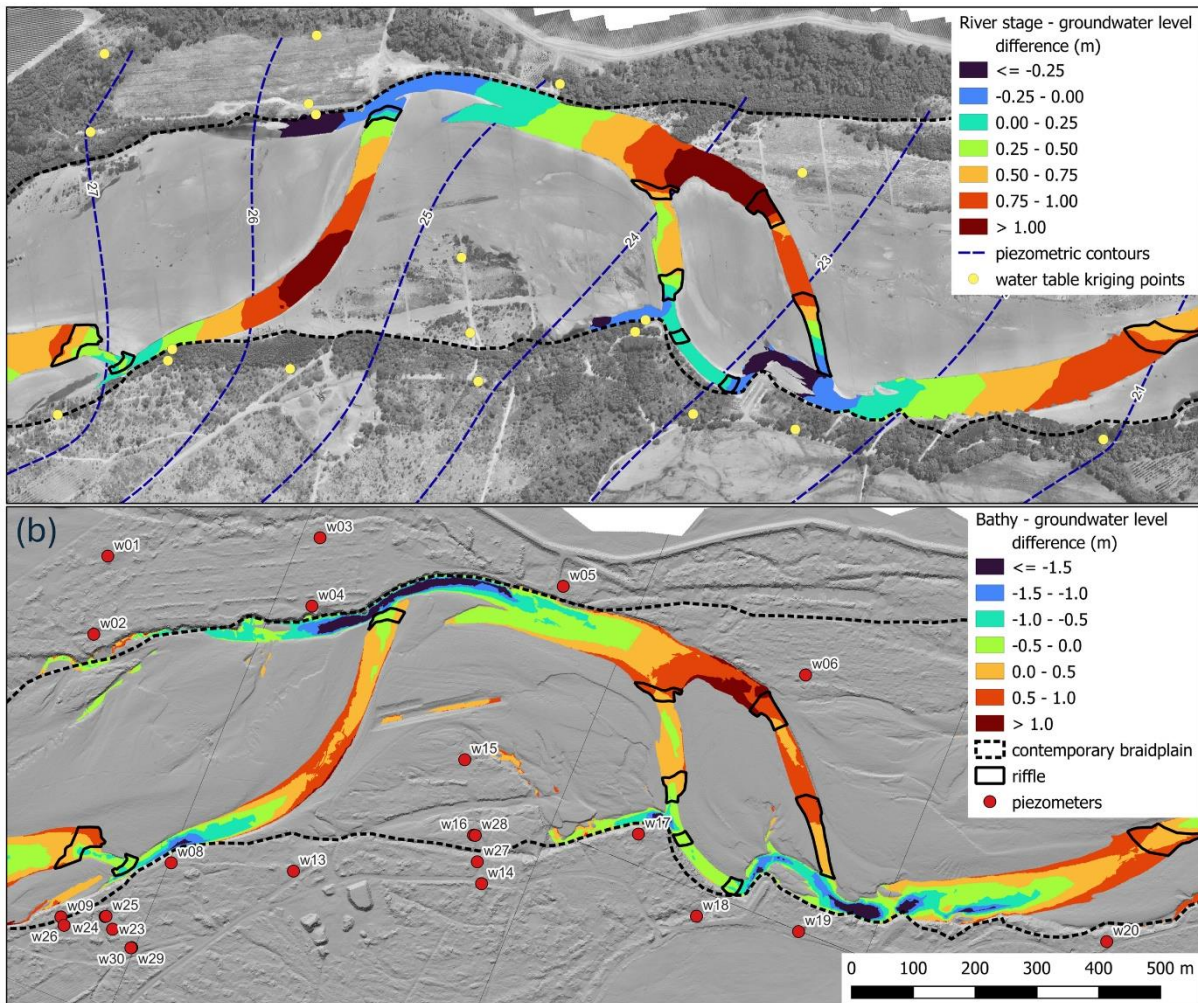
607

608 **Figure 6.** Images of the wetted Wairau River channel showing differences between (a) river

609 water surface and a kriged hydraulic head (overlain on aerial imagery), and (b) bathymetry

610 and kriged hydraulic head (overlain on the DEM). River flow is from left to right.

611

612 *5.3 Water levels and temperature monitoring*

613 Hydraulic heads within the braidplain aquifer are dynamic and fluctuate in response to

614 changes in river stage. Figure 7 shows heads for the Waikirikiri field site, where the base of

615 the BPA is at approximately 207m elevation, and the regional water table is >13m below the

616 unconformity. The variably saturated zone (pore water pressure below saturation) is at least

617 10m thick. For a river system that is hydraulically connected to the regional aquifer, the

618 pressure response outside of the BPA is also dynamic and shows a similar response to the

619   BPA (Figure 7). For a river system with a hydraulic disconnection, the variably saturated

620   zone attenuates the pressure fluctuations in the regional aquifer (Figure 7). The relative

621   water level depth and hydraulic response in the regional aquifer can therefore provide a

622   useful test for hydraulic connectivity between the two aquifer systems.

623
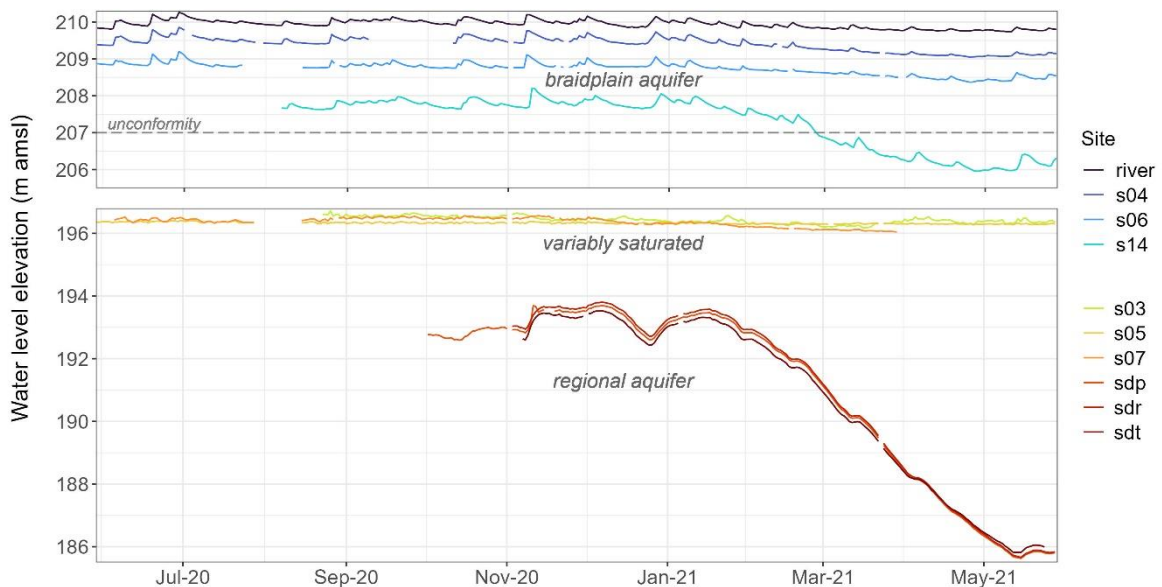
624

625   **Figure 7.** Water level time series data for the Waikirikiri River and braidplain and regional

626   aquifers. Note the vertical offset in the two graphs is due to the thick variably saturated

627   zone beneath the braidplain and regional aquifer. Site locations are shown in Figure 3.

628

629   Data from the Ngaruroro reach show characteristics of a regional aquifer that is both

630   hydraulically connected to the BPA and either disconnected or transitional (Figure 8). These

631   data have been normalised by the median water level to highlight relative changes in

632   response. The BPA site (ng07) responds similarly to the river stage but has a slower

633   recession rate due to storage in the gravels. The two sites that are screened in the regional

634   aquifer (ng02, ng04) are both located 150 m adjacent to and downgradient of the

635   contemporary braidplain (see Figure 3). The upstream site, ng04, has the most rapid

636   recession rate and its peak response is slightly delayed compared to ng02 which responds

637   similarly to the river channel stage. This suggests that this upstream section of the study

638   reach may be hydraulically disconnected or transitional from the regional aquifer (assuming

639   similar hydraulic properties throughout the regional aquifer). The water levels in ng04 are

640   up to 2.4 m below the BPA base (mean 1.8 m) assuming a BPA thickness of 1.6 m below

641   mean river bed level at this site. During flood flow events, the regional aquifer water level

642   ng04 does rise above the river bed elevation, indicating saturated conditions do temporarily

643   occur during flooding.

644
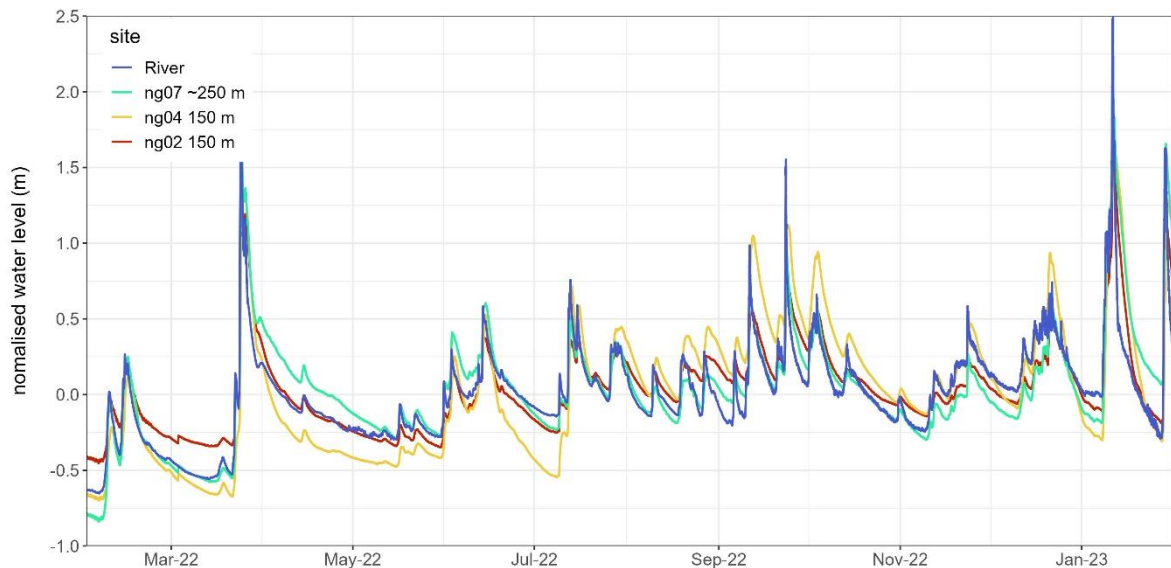
645

646   **Figure 8.** Normalised water level time series data for the Ngaruroro River, braidplain (ng07)

647   and regional aquifers (ng02, ng04). Site locations are shown in Figure 3. Distances in the

648   legend indicate the down gradient distance from the nearest active river channel.

649

650   Figure 9 shows daily average temperatures from representative hydrological settings in each

651   study reach, and the lateral distance downgradient of the nearest active river channel. For

652   sites located within the BPA, temperature responses are similar to the river channel, and

653   driven by individual flow events (ng07, w09, s06). However, event-driven responses can be

654   attenuated, and the season response delayed, at large distances from a channel (s25). Note

655   also that s06 becomes more responsive after a flood event on 30 May 2021 which has

656   changed connectivity between the river and groundwater in this piezometer.

657   For sites within the regional aquifer (ng02, ng04, w12, w21, sdp), the event-driven response

658   is difficult to detect, and the seasonal response depends on the hydraulic relationship

659   between the braidplain and regional aquifers. Sites ng02 and ng04 are equidistant from the

660   Ngaruroro BPA, however ng04 is in a position where the base of the braidplain gravels and

661   regional water table are approximately 1.8m apart, potentially with an intervening variably

662   saturated zone, whereas at ng02 the braidplain and regional aquifers are hydraulically

663   connected. This difference in hydrologic condition may explain the delayed seasonal

664   response in ng04. In the Waikirikiri system, the variably saturated zone is considerably

665   thicker (about 12m), which almost completely attenuates the seasonal temperature

666   response in the regional aquifer.

667

668 **Figure 9.** Representative temperature time series for the three study sites. Piezometer

669 locations are shown in Figure 3, sites ng07, w09, s06 and s25 are screened in the BPA.

670

671 In the Waikirikiri and Ngaruroro river systems, the temperature signals propagate efficiently

672 from river channels to the BPA compared to the regional aquifer. This highlights the

673 distinction between these two aquifers, with the BPA acting as an intermediary in

674 groundwater – surface water exchanges.

675

676 *5.4 Radon-222 sampling*

677 A summary of the radon-222 results and measurement uncertainties for surface water and

678 groundwater sources in the Wairau and Waikirikiri reaches is shown in Table 3. In the

679 Wairau system, samples from riverbed piezometers and riverbed seepages have similar

680 radon activities with ranges 1724-2849 BQ.m^{-3} and 368-2585 BQ.m^{-3} respectively.

681 Accordingly, samples from seepages and riverbed piezometers are both considered to

682 represent the braidplain aquifer.

683 The radon data show distinct groupings, with radon-222 activities increasing from river

684 channel to BPA to regional aquifer. At both sites, radon activities in river run samples were

685 significantly lower than those in BPA samples. In the Wairau study reach, there is a notable

686 overlap in radon activities between the braidplain and regional aquifers, indicating a likely

687 hydraulic connection between these two systems. Conversely, in the Waikirikiri study reach,

688 there is a downward increase in radon activities from the BPA to the variably saturated zone

689 and further into the regional aquifer, with no overlapping values. This suggests a hydraulic

690 disconnection between the BPA and the regional aquifer in the Waikirikiri reach.

691

692 **Table 3.** Measured radon-222 activities and one standard deviation uncertainties (BQ.m^{-3})

693 for the Wairau and Waikirikiri study reaches.

River	Wairau			Waikirikiri			
Sample source	River run	Braidplain aquifer	Regional aquifer	River run	Braidplain aquifer	Variably saturated glacial outwash sediments	Regional aquifer
Samples	14	11	21	10	38	7	6
Rn min	260 ± 85	368 ± 150	739 ± 272	384 ± 185	1791 ± 481	7017± 3607	16111 ± 3305
Rn max	604 ± 224	2849 ± 826	5700 ± 629	809 ± 443	9545 ± 1378	14654 ± 4338	22655 ± 2221
Rn mean	395 ± 180	1307 ± 361	3263 ± 666	568 ± 356	4569 ± 1002	11814 ± 2589	19184 ± 2763

694

695 The determination of residence times between the river and each aquifer depends on

696 knowing the initial channel condition, representative secular equilibrium for the host gravel

697 deposit, as well as a well-defined flow path length. Our estimate of the initial river channel

698 condition is 260 BQ.m^{-3} for Wairau and 380 BQ.m^{-3} for Waikirikiri, reflecting the lowest

699 measured river radon-222 activities. A secular equilibrium estimate of 5000 BQ.m^{-3} was

700 derived for Wairau aquifer samples by plotting measured groundwater radon activity

701 against distance of the piezometer from the river and fitting the ingrowth equation to the

702 data to determine the 21 day equilibrium value. This exercise indicated that the Wairau BPA

703 activities are too low for samples to reach equilibrium. In the absence of sediment specific

704 data, the Wairau aquifer secular equilibrium was chosen to represent the Wairau BPA

705 equilibrium. The secular equilibrium for the Waikirikiri BPA is estimated at approximately

706 8500 BQ.m^{-3} based on the lowest activity observed in porewater samples from piezometer

707 sumps in the variably saturated glacial outwash gravels beneath the braidplain aquifer (7017

708 BQ.m^{-3}), and the highest activity observed in the BPA (9545 BQ.m^{-3}). Based on the secular

709 equilibrium values chosen, residence times for our study reach samples are estimated to be

710 in the range of 0.1 to 4.4 days for the Wairau BPA in the study reach and 1 to >12 days for

711 the Waikirikiri BPA. Due to the large uncertainties associated with the WAT250 method,

712 these estimates should be considered for comparative purposes only.

713

714 *5.5 Geophysics*

715 ERT surveys of the contemporary braidplain in the Wairau and Waikirikiri reaches yielded

716 varying degrees of success. The surveys that returned the most consistent subsurface

717 resistivity response were conducted in the river channel itself, due to the presence of water

718 in the near surface, which improved the connection between electrodes and the underlying

719 resistive substrate. Figure 10 shows dipole-dipole array resistivity profiles across a braid of

720 the Wairau (~ 30 m wide), and two braids of the Waikirikiri (~40 m wide). These profiles

721 reveal the contact between the braidplain aquifer and underlying sediments (the

722 unconformities shown in Fig. 4) at elevations consistent with drillhole coring. For

723 comparison, the elevation of the same unconformity, derived by kriging intercepts of the

724 BPA base within the contemporary braidplain (Figure 3.), is shown in red in Figure 10. The

725 two profiles are shown at the same spatial and resistivity scale, and an interpretation has

726 been made based on drilling information. Both profiles show a contrast between resistive

727 (~1000 ohm-m) loose sandy gravels that host the BPA, and the underlying lower resistivity

728 (<800 ohm-m) associated with older, very poorly sorted sediments. The Wairau profile

729 reveals the unconformity at the base of the active braidplain gravels as a less resistive layer

730 at ~19.5 m elevation, and a saturated BPA thickness of ~3.5 m. On the Waikirikiri profile, the

731 unconformity at the base of the braidplain gravels lies at ~207.5 m elevation, and the

732 saturated thickness of the BPA is only 2-2.5 m. The underlying very poorly sorted glacial

733 outwash gravels typically show relatively low resistivities (≤ 600 ohm-m) due to the relative

734 abundance of clay-sized sediment, even when not fully saturated.

735
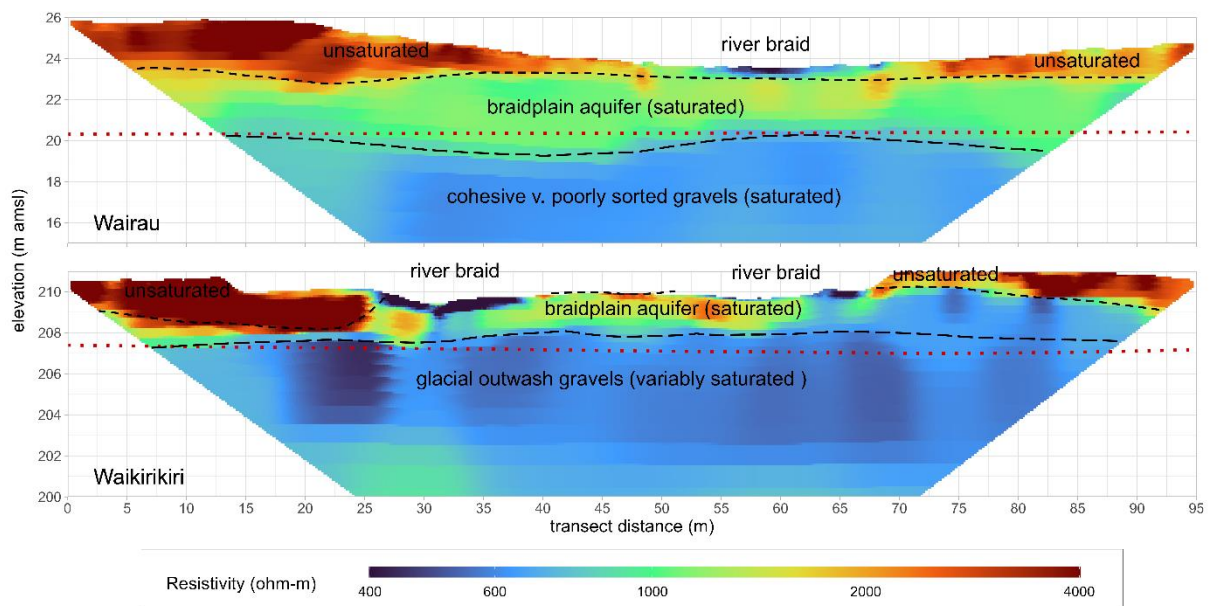
736

737 **Figure 10.** Subsurface resistivity collected by Electrical Resistivity Tomography (ERT) across

738 Wairau and Waikirikiri river braids, looking downstream. Surfaces interpreted from the

739 resistivity data are shown in black. An interpolated surface for the base of the BPA derived

740 from drilling and bed data is shown in red.

741

5.6 Passive and active distributed temperature sensing

The hydrogeologic structure in the Wairau study reach has been assessed by monthly DTS

and ADTS surveys (Figure 11) conducted on a vertically installed fibre optic cable located 20

m from the active braidplain margin (w27 in Figure 3). While w27 lies just outside of the

existing engineered contemporary braidplain, this site does contain remnant braidplain

sediments deposited prior to stabilisation of the river margins in the 1960s. The timing of

the DTS surveys with respect to river temperature is shown in Figure 11c. The survey

temperature profiles show consistent inflections with depth due to the attenuation of the

river recharge temperature response through saturated sediments of contrasting hydraulic

conductivity (Figure 11). These inflections correspond to the depths where a change in

sediment characteristics can be seen in the bore log, manifest as progressively increased

sediment cohesion, poorer sorting, and increasing silt and clay content with depth. In the

DTS profile, the older silty clay-bound and indurated sediments have a large influence on

subsurface flow, i.e., a reduction in flow through this material.

756

757
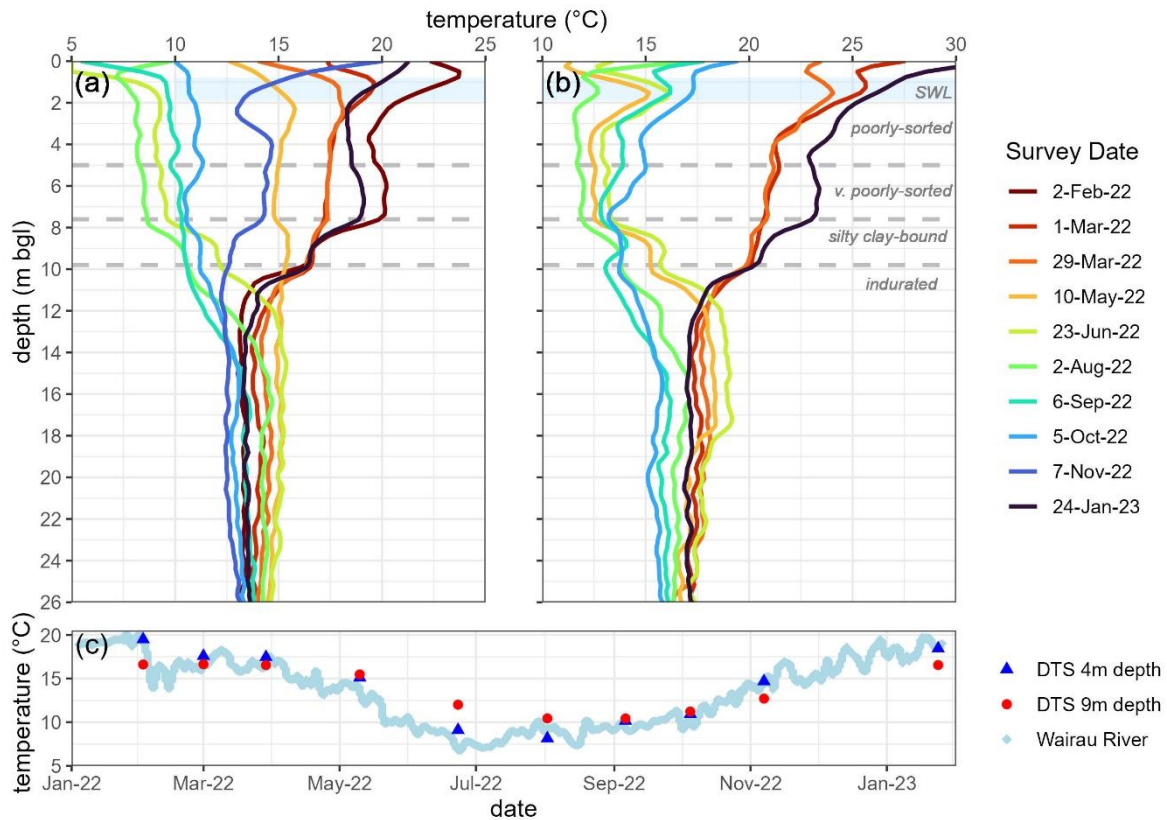
Figure 11. Vertical (a) distributed temperature sensing (DTS) and (b) active-distributed

temperature sensing (A-DTS) surveys conducted on the south bank of the Wairau River on

w27. The river temperature over the period of the surveys is shown in (c) along with

temperatures measured by DTS at 4 and 9 m depth. SWL=static water level measurements

over the survey period

763

6.0 Characteristics of the identified braidplain aquifers

A summary of the approximate dimensions and potential maximum groundwater storage

volumes of the three braidplain aquifers investigated is shown in Table 4. In all three

reaches, the BPA is laterally extensive, but very thin.

768   The Wairau River has the greatest BPA storage potential, largely due to its observed

769   saturated thickness of up to 4.1 m. However, the Wairau is also a highly channelised river,

770   and has a large bathymetric range, giving its BPA a large potential variability in saturated

771   thickness in response to river channel stage fluctuations. Of significance for water

772   management in the Wairau Plain is that the very poorly sorted gravels are thin beneath the

773   Wairau contemporary braidplain and underlain by buried fans of silty clay-bound and

774   indurated gravels which act as a vertical flow barrier (see Figure 10). Gravel extraction from

775   the river system has dropped the mean bed level by approximately 1 m within our study

776   reach since the early 1990s (Gardner and Sharma, 2016). This has allowed the river to

777   rework sediment to greater depths, which has thinned and reduced the effective

778   transmissivity of the gravel sequence overlying the buried fan deposits in addition to

779   reducing the hydraulic gradient between the river system and regional aquifer.

780

781   **Table 4.** Dimensions and maximum storage volumes of braidplain aquifers observed in the

782   three study areas.

River	Approximate width (m)	Contact depth (m) min-max (mean)	Porosity min-max (mean)	Storage volume ($m^3.m^{-1}$)
Ngaruroro	300	1.2 - 2.4 (1.6) n=4	0.12-0.35 (0.21) n=9	80-150
Wairau	450	2.4– 5.7 (4.1) n=6	0.09-0.46 (0.22) n=21	210-500
Waikirikiri	400	2.0 - 3.7 (2.8) n=16	0.09-0.22 (0.14) n=9	130-240

783

7.0 Discussion

785   The proposed conceptualisation enables a complex braided river system of high complexity

786   to be represented by a few key hydrogeological elements. These are represented in Figure 1

787   as a contemporary braidplain, the margins of which mark the lateral extent of the braidplain

788   aquifer (1), an underlying unconformity with more consolidated and more poorly sorted

789 sediments (2), and observations of the hydraulic relationship between the braidplain and

790 regional aquifers (a or b). For braided rivers, this approach integrates existing concepts of an

791 alluvial aquifer, and hydrological hyporheic and parafluvial zones into a single

792 conceptualisation of the contemporary braidplain subsurface. By identifying the base and

793 margins of the BPA, and the process which forms it (reworking of bed material), the vertical

794 and lateral extents to which hyporheic and parafluvial exchange occur can be identified by a

795 change in sediment characteristics.

796

797 Point-scale features of braided rivers are described well by the existing hydrological

798 framework proposed by Fox and Durnford (2003) and modified by Brunner et al. (2009a and

799 b). Under this framework, individual channels can be considered as hydrologically connected

800 (gaining or losing), disconnected (losing), or transitional (losing). However, this framework

801 starts to break down for braided rivers at local to sub-catchment scales, as all four of these

802 hydrological states can occur along a single cross-section of the braidplain regardless of

803 whether the river has a net gain or loss. However, at the reach or sub-catchment scale, a

804 braided river can be considered a *river system*, which can be described by any one of those

805 hydrological states in relation to the regional groundwater system. For example, a river

806 braidplain reach can be hydrologically disconnected and be losing water to groundwater

807 overall, even though individual channels are hydrologically connected and locally gaining

808 flow from BPA groundwater. The conceptualisation posed by Fox and Durnford (2003) can

809 therefore be applied to different scales within a braided river system, but its application,

810 and therefore interpretation of field measurements, requires knowledge of subsurface

811 structure and saturation.

812

813   The difference in sediment characteristics above and below the unconformity at the base of

814   the BPA indicates that the process of BPA formation is controlled by the mobilisation of bed

815   material during flood flows, which loosen and sort the braidplain gravels, and winnow the

816   finer fraction. This process of gravel mobility associated with flood events is supported by

817   bathymetric observations of the depth of river channel scouring in deeper pools which

818   agrees with the depths of the unconformity in core data. In the absence of drill core and

819   particle size distribution data, we suggest that the elevation of pool depths measured soon

820   after a flood event can be used to approximate the base of the BPA. This will only provide a

821   minimum depth of the BPA base since the river is expected to deposit some sediment in

822   scoured areas during the flow recession. The thickness of a river's BPA is likely to depend on

823   the inter-relationship between several factors, including contemporary braidplain width,

824   sediment characteristics and the balance of sediment supply, the frequency and magnitude

825   of peak flow events, and the use of "hard engineering" to control a river's position. While

826   some of these factors are natural, the factors related to width and depth are influenced by

827   river engineering applied at each river. The Wairau River has the thickest BPA and has the

828   highest hydrological energy of the reaches studied. This river is considered by some river

829   engineers to be excessively narrowed, and a wider contemporary braidplain may result in a

830   dispersion of energy during flood flows, and subsequent thinning of the BPA. Interestingly,

831   the Ngaruroro River is also subject to high peak flows, although bed mobilising flows occur

832   less frequently than the Wairau. It is likely that the Ngaruroro BPA is being thinned by the

833   large volume of gravel extraction occurring within the study reach.

834

835   The LiDAR and bathymetric data gathered from our three study sites indicate that individual

836   river channels locally merge with and diverge from the water table surface of the BPA.

837   Water exchange across the bed is determined by bathymetry and hydraulic properties,

838   where the river can be forced above the water table by gravel lobes or dropped into the

839   water table in locations of scouring. Areas of relatively still water (pools) are therefore the

840   surface expression of the BPA, with seeps representing locations where the bedform drops

841   below the level of the BPA water table. This explains the occurrence of higher radon-222

842   activities in pools compared to flowing river channels, as well as differences in seasonal

843   water temperature.

844

845   For the interpretation of field data, the proposed conceptualisation highlights the

846   importance of identifying and knowing the nature of the relationship between these three

847   potential water sources to interpret observations. For example, to understand the nature

848   and magnitude of river-aquifer interaction by only sampling radon-222 in river channels can

849   be misleading. This is because the radon activity measured in the river depends both on the

850   river setting (run or pool), and the nature of the interaction between the BPA and regional

851   aquifer.

852

853   From a modelling perspective, it is questionable if a streambed conductance term is an

854   appropriate physical mechanism for representing braided river-aquifer exchange at the local

855   or catchment scale. The role of bed conductance, if significant, is to regulate exchange

856   between individual river channels and the BPA. Due to the relatively high transmissivity of

857   the bed materials, hyporheic exchange is an integral process of braided river flow, and

858   water can be seen to freely exchange between the surface and the bed. It follows that

859   consideration of water storage in the bed sediments (BPA) with a conductance term to

860   impede flow beneath those sediments would be a more appropriate approach for

861 simulating braided rivers at larger scales than to simulate individual channels with bed

862 conductance.

863

864 The BPA concept resolves vague definitions of "groundwater" in groundwater – surface

865 water interactions in braided rivers by considering the river as a whole system with an

866 associated subsurface storage component distinct from the regional groundwater system.

867 This provides specificity to the concept of a "river corridor" (Harvey and Gooseff, 2015),

868 where a river comprises not just the river channels, but the surrounding, fluvial deposits,

869 riparian zones, and floodplains between which hydrologic exchange occurs.

870

871 Braided river systems are spatially and temporally variable, which introduces heterogeneity

872 both within a BPA, and the adjacent older sediments. This heterogeneity can manifest as

873 preferential flowpaths, which can influence exchange fluxes at a local scale, as evident in

874 spatial variability of temperature and radon data. While the BPA consists of high

875 transmissivity sediments, and can itself be considered a preferential flow path at the

876 regional scale, the presence of preferential flow within the BPA at the local scale is not

877 captured by the conceptualisation presented here. We therefore recommend application of

878 the BPA concept at the regional scale, and to provide a hydrogeological context for local

879 scale studies. An additional consideration for applying the BPA concept is the volume of

880 reworked material associated with the river. In braided river environments, the volume of

881 gravel associated with the BPA is large, and significantly greater than the wetted channel

882 volume at average flow conditions. However, in some gravel bed rivers, the volume of

883 sediment mobilised by flooding events could potentially be very thin, and the relevance of

884 these mobile sediments on the exchange between the river and regional groundwater

885 system will depend on the scale of the study.

886 At the regional scale, the BPA concept is best applied to braided rivers that have stable or

887 actively degrading beds, or have had some form of bank stabilisation, which is common

888 where flooding is considered a risk to adjacent land. Stabilisation of river margins serves to

889 increase the frequency of gravel remobilisation within the active braidplain and prevent

890 reworking of adjacent bed material that may be part of the historical braidplain. Fine

891 sediment can percolate through the gravels or be deposited on the surface, and if these

892 gravels are not subsequently reworked, this can gradually consolidate and potentially clog

893 the pore spaces, accentuating the difference between contemporary and adjacent historical

894 braidplain sediments. Narrowing the area of braidplain that is reworked can thereby narrow

895 the BPA. The conceptualisation may be less appropriate, or the BPA boundaries may be less

896 distinct, where the contemporary braidplain margins are much wider than the active

897 braidplain and reworked over longer timeframes. This type of braided river behaviour is

898 typically seen in mountainous areas with low land use pressure, for example in the Southern

899 Alps of New Zealand, but would have occurred on lowland plains prior to widespread

900 engineering of river margins in New Zealand during the 1960s. If river channels can adjust

901 laterally over a wider area, it is expected that sediments within the contemporary braidplain

902 will be more heterogeneous, with channels of permeable recently mobilised gravel

903 intermingled with islands/areas of varying age and permeability. In these cases, the extent

904 of the BPA beyond the active braidplain across the contemporary braidplain may depend on

905 the frequency of contemporary braidplain reworking, or the connectivity with the active

906 braidplain. Similarly, it would be difficult to detect the base of the BPA in situations where

907 the river bed is rapidly aggrading.

908

8.0 Conclusions

910 By investigating the surface and subsurface sediment and saturation in three study reaches,

911 we have developed a conceptualisation of how braided rivers exchange water at the local

912 (reach) and sub-catchment (aquifer) scale. The interaction between the river system and

913 groundwater can be considered to occur between (a) individual river channels and the BPA

914 (hyporheic and parafluvial exchange), or (b) the braidplain and regional aquifers. Central to

915 this conceptualisation is the presence of a braidplain aquifer (BPA), a thin (2-5 m) layer of

916 loose, poorly sorted gravel which is formed via the process of bed mobilisation during flood-

917 flows. The base of the BPA can be identified in drill core as an unconformity between poorly

918 sorted unconsolidated gravels overlying more consolidated very poorly sorted gravels.

919 Individual river channels can be hydraulically connected, transitional, or disconnected from

920 the BPA, depending on the relationship between the braidplain water table and bathymetry.

921 The nature of the hydraulic relationship between the braidplain and regional aquifers can

922 also be hydraulically connected, transitional, or disconnected, depending on the relationship

923 between the regional water table and base of the BPA gravels. Approaching the braided

924 river as a (whole) system (river and BPA combined) enables field data to be interpreted

925 within the context of its water source.

926

927 From a modelling perspective, the conceptualisation enables rivers to be appropriately

928 represented at a local scale (river-BPA), or a regional scale (BPA/river system-regional

929 aquifer), depending on the modelling objective. A parallel investigation not presented here

930 is focussed on the implementation of the proposed conceptualisation into sub-catchment

931   scale models to quantify how changes in river morphology and BPA storage influence

932   recharge to the regional groundwater system. A key research gap is to understand the

933   relationship between BPA dimensions, bathymetry, and river flow dynamics, and this is a

934   subject for future research.

935

936   **Acknowledgements**

937   The authors would like to thank the New Zealand Ministry of Business, Innovation and

938   Employment for funding this research through the project "Subsurface processes in braided

939   rivers - hyporheic exchange and leakage to groundwater". We are also grateful to additional

940   support from Hawkes Bay Regional Council, Marlborough District Council and Environment

941   Canterbury. We also acknowledge the contribution of the Hydrogeophysics Group, Aarhus

942   University who carried out the EM surveys on our rivers, and Christy Songola who did the

943   radon sampling and analysis at our Selwyn study site. Lastly, we would like to express our

944   gratitude to the reviewers for their valuable comments, which helped us improve the

945   quality of this article.

946

947   **Financial support**

948   This research has been supported by the Ministry of Business, Innovation and Employment

949   (grant no. LVLX1901).

950

951   **References**

952   Anderson, E.I. (2005) Modeling groundwater–surface water interactions using the Dupuit

953   approximation. *Advances in Water Resources* 28(4), 315-327.

954   Banks, E.W., Simmons, C.T., Love, A.J., and Shand, P. (2011). Assessing spatial and temporal

955   connectivity between surface water and groundwater in a regional catchment: Implications

956   for regional scale water quantity and quality. *Journal of Hydrology*, 404(1-2): p. 30-49,

957   doi:10.1016/j.jhydrol.2011.04.017.

958   Banks, E.W., Morgan, L.K., Sai Louie, A.J., Dempsey, D., Wilson, S.R. (2022). Active

959   distributed temperature sensing to assess surface water-groundwater interaction and river

960   loss in braided river systems. *Journal of Hydrology 615*, 128667,

961   doi:10.1016/j.jhydrol.2022.128667

962   Barthel, R., Banzhaf, S. (2016). Groundwater and Surface Water Interaction at the Regional-

963   scale - A Review with Focus on Regional Integrated Models. *Water Resources Management*

964   *30*: 1–32, doi:10.1007/s11269-015-1163-z

965   Bayat, H., Rastgo, M., Mansouri Zadeh, M., Vereecken, H. (2015). Particle size distribution

966   models, their characteristics and fitting capability. *Journal of Hydrology* 529, 872-889,

967   doi:10.1016/j.jhydrol.2015.08.067

968   Begg, J.G, Johnston, M.R. (compilers) (2000). Geology of the Wellington area. Institute of

969   Geological & Nuclear Sciences 1:250 000 geological map 10. 1 sheet + 64p. Lower Hutt, New

970   Zealand. GNS Science.

971   Boano, F., Harvey, J.W., Marion, A. Packman, A.I., Revelli, R., Ridolfi, L., Wörman, A. (2014).

972   Hyporheic flow and transport processes: Mechanisms, models, and biogeochemical

973 implications. *Reviews of Geophysics 52*: 603–679, doi:10.5194/hess-22-1917-

974 201810.1002/2012RG000417

975 Boano, F., Revelli, R., Ridolfi, L. (2008). Reduction of the hyporheic zone volume due to the

976 stream-aquifer interaction. *Geophysical Research Letters 35*: L09401,

977 doi:10.1029/2008GL033554.

978 Booker, D. J. (2013). Spatial and temporal patterns in the frequency of events exceeding

979 three times the median flow (FRE3) across New Zealand. *Journal of Hydrology (NZ) 52*, 15-

980 39.

981 Boulton, A.J., Findlay, S., Marmonier, P., Stanley, E.H., Valett, H.M. (1998). The functional

982 significance of the hyporheic zone in streams and rivers. *Annual Review of Ecology &*

983 *Systematics 29*: 59–81, doi: 10.1146/annurev.ecolsys.29.1.59

984 Bourke, S.A., Cook, P.G., Shanafield, M., Dogramaci, S., Clark, J.F. (2014). Characterisation of

985 hyporheic exchange in a losing stream using radon-222. *Journal of Hydrology 519*: 94–105,

986 doi:10.1016/j.jhydrol.2014.06.057.

987 Bristow, C.S., Best, J.L. (1993) Braided rivers: perspectives and problems. From: Best, J.L. and

988 Bristow, C.S. (eds) *Braided Rivers*, Geological Society, London, Special Publications. Volume

989 75 Pages 1-11, doi:10.1144/GSL.SP.1993.075.01

990 Brower, A., Hoyle, J., Gray, D., Buelow, F., Calkin, A., Fuller, I., Gabrielsson, R., Grove, P.,

991 Brierley, G., Sai-Louie, A.J., Rogers, J., Shulmeister, J., Uetz, K., Worthington, S., Vosloo, R.

992 (2024). New Zealand's braided rivers: The land the law forgot. *Earth Surface Processes and*

993 *Landforms 49 (1)*: 10–14, doi: 10.1002/esp.5728

994   Brunner, P., Cook, P.G., Simmons, C.T., (2009a), Hydrogeologic controls on disconnection

995   between surface water and groundwater, *Water Resource. Res*., 45(1), 1–13, W01422,

996   doi:10.1029/2008WR006953

997   Brunner, P., Simmons, C.T., Cook, P.G. (2009b). Spatial and temporal aspects of the

998   transition from connection to disconnection between rivers, lakes and groundwater. *Journal*

999   *of Hydrology 376* (1–2): 159–169, doi:10.1016/ j.jhydrol.2009.07.023.

1000   Brunner, P., Simmons, C.T. (2012). Hydrogeosphere: A Fully Integrated, Physically Based

1001   Hydrological Model. *Groundwater 50*: 170-176, doi:10.1111/j.1745-6584.2011.00882

1002   Brunner, P., Therrien, R., Renard, P., Simmons, C.T., Hendricks Franssen, H.-J. (2017).

1003   Advances in understanding river-groundwater interactions. *Reviews of Geophysics 55*: 818-

1004   854 doi:10.1002/2017RG000556

1005   Cardenas, M.B., Zlotnik, V.A. 2003. Three-dimensional model of modern channel bend

1006   deposits. *Water Resources Research 39*: 1141, doi:10.1029/2002WR001383

1007   Cartwright, I., Hoffmann, H. 2016. Using radon to understand parafluvial flows and the

1008   changing locations of groundwater inflows in the Avon River, southeast Australia. *Hydrology*

1009   *& Earth Systems Sciences 20*: 3581–3600, doi:10.5194/hess-20-3581-2016

1010   Coluccio, K., Morgan, L. K. (2019). A review of methods for measuring groundwater-surface

1011   water exchange in braided rivers. *Hydrology & Earth Systems Sciences 23*: 4397–4417,

1012   doi:10.5194/hess-23-4397-2019

1013   Di Ciacca, A., Leterme, B., Laloy, E., Diederik, D., Vanderborght, J. (2019). Scale-dependent

1014   parameterization of groundwater–surface water interactions in a regional hydrogeological

1015   model. *Journal of Hydrology 576*: 494-507, doi:10.1016/j.jhydrol.2019.06.072.

1016   Di Ciacca, A., Wilson, S., Kang, J., Wöhling, T. (2023). Deriving transmission losses in

1017   ephemeral rivers using satellite imagery and machine learning. *Hydrology & Earth Systems*

1018   *Sciences 27*: 703-722, doi:10.5194/hess-27-703-2023

1019   Dravid P.N., Brown L.J., 1997. Heretaunga Plain Groundwater Study - Vol 1: Findings.

1020   Hawke's Bay Regional Council, 254p.

1021   Durejka, S., Gilfedder, B., Frei, S. (2019). A method for long-term high resolution 222Radon

1022   measurements using a new hydrophobic capillary membrane system. *Journal of*

1023   *Environmental Radioactivity 208-209*: 105980, doi:10.1016/j.jenvrad.2019.05.012.

1024   Durridge (2020a). RAD7 electronic radon detector user manual.

1025   Durridge (2020b). RAD H2O Radon in Water accessory for the RAD7 User Manual.

1026   Durridge (2020c). Continuous Radon in Water Accessory for the RAD7 user manual.

1027   Durridge. (2021). DRYSTIK Models ADS-3 andADS-3R Active Moisture Exchanger Accessory

1028   for the RAD7 User Manual

1029   Folk R.L., Ward W.C., 1957. Brazos River bar: a study in the significance of grain size

1030   parameters. *Journal of Sedimentary Petrology 27*: 3–26.

1031   Forsyth, P.J., Barrell, D.J.A., Jongens, R. (compilers) (2008). Geology of the Christchurch area.

1032   Institute of Geological & Nuclear Sciences 1:250 000 geological map 16. 1 sheet + 67p.

1033   Lower Hutt, New Zealand. GNS Science.

1034   Fox, G.A., Durnford, D.S., 2003. Unsaturated hyporheic zone flow in stream conjunctive

1035   systems. *Advances in Water Resources* 26 (9), 989–1000.

1036   Gardner, M., Sharma, N., 2016. Wairau River Mean Bed Level and Volumetric Analysis: 2010

1037   to 2016. Report to Marlborough District Council, 57p.

1038   González-Pinzón, R., Ward, A.S., Hatch, C.E., Wlostowski, A.N., Singha, K., Gooseff, M.N.,

1039   Haggerty, R., Harvey, J.W., Cirpka, O.A., Brock, J.T. (2015). A field comparison of multiple

1040   techniques to quantify groundwater-surface-water interactions. *Freshwater Science 34*: 139-

1041   160, doi:10.1086/679738

1042   Gray DP, Hicks M, Greenwood M 2016. Advances in geomorphology and aquatic ecology of

1043   braided rivers. In Jellyman PG, Davie TJA, Pearson CP, Harding JS. (Eds) Advances in New

1044   Zealand freshwater science. New Zealand Freshwater Sciences Society, Christchurch, New

1045   Zealand. Pp 357-378.

1046   Harbaugh, A.W. (2005). MODFLOW-2005, the U.S. Geological Survey modular ground-water

1047   model -- the Ground-Water Flow Process: U.S. Geological Survey Techniques & Methods 6-

1048   A16.

1049   Harvey, J., Gooseff, M. (2015). River corridor science: Hydrologic exchange and ecological

1050   consequences from bedforms to basins. *Water Resources Research 51*: 6893–6922,

1051   doi:10.1002/2015WR017617.

1052   Harvey, J.W., Wagner, B.J. (2000). Quantifying Hydrologic Interactions between Streams and

1053   Their Subsurface Hyporheic Zones. In: Jones, J.B. and Mulholland, P.J. (eds) Streams and

1054   ground waters. San Diego, CA: Academic Press, pp. 3–44, doi: 10.1016/B978-012389845-

1055   6/50002-8.

Holmes, R. M., Fisher, S. G., & Grimm, N. B. (1994). Parafluvial Nitrogen Dynamics in a

Desert Stream Ecosystem. *Journal of the North American Benthological Society, 13 (4)*: 468–

478, doi:10.2307/1467844

Huber, E., Huggenberger, P. (2016). Subsurface flow mixing in coarse, braided river deposits.

Hydrology & Earth Systems Sciences 20: 2035–2046, doi:10.5194/hess-20-2035-2016

Huggenberger, P., Hoehn, E., Beschta, R., Woessner, W. (1998). Abiotic aspects of channels

and floodplains in riparian ecology. *Freshwater Biology 40*: 407-425, doi:10.1046/j.1365-

2427.1998.00371.x

Huggenberger P., Regli, C. (2006). A sedimentological model to characterise Braided River

deposits for hydrogeological applications. In: Sambrook Smith GH (ed) Braided rivers:

process, deposits, ecology and management. Blackwell, Malden, MA, pp 51–74.

Hupp, C.R., Osterkamp, W.R. 1996. Riparian vegetation and fluvial geomorphic processes.

Geomorphology 14: 277-295.

Kalbus, E., Reinstorf, F., Schirmer, M., 2006. Measuring methods for groundwater-surface

water interactions: a review. *Hydrology & Earth System Sciences 10*: 873-887

doi:10.5194/hess-10-873-2006

Khambhammettu, P., Renard, P., & Doherty, J. (2020). The traveling pilot point method. A

novel approach to parameterize the inverse problem for categorical fields. *Advances in*

Water Resources 138: 103556, doi:10.1016/j.advwatres.2020.103556.

Larned, S. T., Hicks, D. M., Schmidt, J., Davey, A. J. H., Dey, K., Scarsbrook, M., Arscott, D. B.,

Woods, R. A. (2008). The Selwyn River of New Zealand: A benchmark system for alluvial

plain rivers. *River Research & Applications 24*, 1–21, doi:10.1002/rra.1054

1078   Laube, G., Schmidt, C., Fleckenstein, J.H. (2018). The systematic effect of streambed

1079   conductivity heterogeneity on hyporheic flux and residence time. *Advances in Water*

1080   *Resources 122*: 60-69, doi:10.1016/j.advwatres.2018.10.003

1081   Lee, J.M, Bland, K.J., Townsend, D.B., Kamp, P.J. J. (compilers) (2011). Geology of the

1082   Hawkes Bay area. Institute of Geological & Nuclear Sciences 1:250 000 geological map 8. 1

1083   sheet + 93p. Lower Hutt, New Zealand. GNS Science.

1084   Levy, J., Birck, M. D., Mutiti, S., Kilroy, K. C., Windeler, B., Idris, O., & Allen, L. N. (2011). The

1085   impact of storm events on a riverbed system and its hydraulic conductivity at a site of

1086   induced infiltration. *Journal of Environmental Management, 92*: 1960–1971,

1087   doi:10.1016/j.jenvman.2011.03.017

1088   Measures, R. (2012). Modelling gravel transport, extraction and bed level change in the

1089   Ngaruroro River. NIWA Client Report CHC2012-121 for Hawkes Bay Regional Council.

1090   Montgomery, J., Bind, J., Measures, R., Hoyle, J. (subm.). Novel methods for measuring

1091   porosity in gravel bed rivers. *Water Resources Research*.

1092   Morel-Seytoux, H.J., Miller, C.D., Mehl, S. and Miracapillo, C. (2018) Achilles' heel of

1093   integrated hydrologic models: The stream-aquifer flow exchange, and proposed alternative.

1094   *Journal of Hydrology* 564, 900-908.

1095   Niswonger, R.G., Prudic, D.E. (2005). Documentation of the Streamflow-Routing (SFR2)

1096   Package to include unsaturated flow beneath streams - A modification to SFR1: U.S.

1097   Geological Survey Techniques and Methods 6-A13, 50 p.

1098   Pirot, G., Huber, E., Irving, J., Linde, N. (2019). Reduction of conceptual model uncertainty

1099   using ground-penetrating radar profiles: Field-demonstration for a braided-river aquifer.

1100   *Journal of Hydrology 571*: 254-264, doi:10.1016/j.jhydrol.2019.01.047

1101   Pirot, G., Straubhaar, J., and Renard, P. (2014). Simulation of braided river elevation model

1102   time series with multiple-point statistics. *Geomorphology 214*: 148–156,

1103   doi:10.1016/j.geomorph.2014.01.022

1104   Pirot, G., Straubhaar, J., Renard, P. (2015). A pseudo genetic model of coarse braided-river

1105   deposits. *Water Resources Research 51*: 9595-9611, doi:10.1002/2015WR017078.

1106   Poole, G.C., Berman, C.H. (2001). An ecological perspective on in-stream temperature:

1107   natural heat dynamics and mechanisms of human-caused thermal degradation.

1108   *Environmental Management 27*: 787-802, doi:10.1007/s002670010188

1109   Pryshlak, T.T., Sawyer, A.H., Stonedahl, S.H., Soltanian, M.R. (2015). Multiscale hyporheic

1110   exchange through strongly heterogeneous sediments. *Water Resources Research 51*: 9127–

1111   9140, doi:10.1002/2015WR017293.

1112   Rawlinson, Z.J, Westerhoff, R.S., Foged, N., Kellett, R.L. (2021). Hawke's Bay 3D Aquifer

1113   Mapping Project: Heretaunga Plains SkyTEM data processing and resistivity models. GNS

1114   Science Consultancy Report 2021/93

1115   Reinfelds, I., Nanson, G. (1993), Formation of braided river floodplains, Waimakariri River,

1116   New Zealand. *Sedimentology 40*: 1113-1127. https://doi.org/10.1111/j.1365-

1117   3091.1993.tb01382.x

1118   Rushton, K. (2007) Representation in regional models of saturated river–aquifer interaction

1119   for gaining/losing rivers. Journal of Hydrology 334(1), 262-281.

1120 Schälchli, U. (1992). The clogging of coarse gravel river beds by fine sediment. *Hydrobiologia*

1121 *235/236(1)*:189–197

1122 Schilling, O. S., Partington, D. J., Doherty, J., Kipfer, R., Hunkeler, D., & Brunner, P. (2022).

1123 Buried paleo-channel detection with a groundwater model, tracer-based observations, and

1124 spatially varying, preferred anisotropy pilot point calibration. *Geophysical Research Letters,*

1125 *49 (14)*: e2022GL098944. https://doi.org/10.1029/2022GL098944

1126 Shanafield, M., Cook, P.G. (2014). Transmission losses, infiltration and groundwater

1127 recharge through ephemeral and intermittent streambeds: A review of applied methods.

1128 *Journal of Hydrology 511*: 518–529, doi:10.1016/j.jhydrol.2014.01.068

1129 Shanafield, M., Bourke, S.A., Zimmer, M.A., Costigan, K.H. (2021). An overview of the

1130 hydrology of non-perennial rivers and streams. *WIREs Water 8*: e1504,

1131 doi:10.1002/wat2.1504Fsongol

1132 Songola, C. (2022). Characterising Surface Water and Groundwater Interactions in Braided

1133 Rivers Using Hydraulics and Environmental Tracers: The Waikirikiri Selwyn River. MSc thesis,

1134 Lincoln University.

1135 Sophocleous, M. (2002). Interactions between groundwater and surface water: The state of

1136 the science. *Hydrogeology Journal 10 (1)*: 52-67, doi:10.1007/s10040-001-0170-8

1137 Stanford, J.A. & Ward, J. V. (1993). An Ecosystem Perspective of Alluvial Rivers: Connectivity

1138 and the Hyporheic Corridor. *Journal of the North American Benthological Society 12 (1)*: 48-

1139 60.

1140 Steiger, J., Tabacchi, E., Dufour, S., Corenblit, D., Peiry, J.-L. (2005), Hydrogeomorphic

1141 processes affecting riparian habitat within alluvial channel–floodplain river systems: a

1142   review for the temperate zone. *River Research and Applications 21*: 719-737,

1143   doi:10.1002/rra.879

1144   Tang, Q., Schilling, O. S., Kurtz, W., Brunner, P., Vereecken, H., & Hendricks Franssen, H.-J.

1145   (2018). Simulating flood induced riverbed transience using unmanned aerial vehicles,

1146   physically-based hydrological modelling and the ensemble Kalman filter. *Water Resources*

1147   *Research 54*: 9342–9363, doi:10.1029/2018WR023067.

1148   Theel, M., Huggenberger, P., Zosseder, K. (2020). Assessment of the heterogeneity of

1149   hydraulic properties in gravelly outwash plains: a regionally scaled sedimentological analysis

1150   in the Munich gravel plain, Germany. *Hydrogeology Journal 28*: 2657–2674,

1151   doi:10.1007/s10040-020-02205-y

1152   Therrien, R., McLaren, R. G., Sudicky, E. A., Panday, S. M. (2010). *HydroGeoSphere: A Three-*

1153   *dimensional Numerical Model Describing Fully-integrated Subsurface and Surface Flow and*

1154   *Solute Transport*. Groundwater Simulations Group, University of Waterloo. 443 p.

1155   Valett, H.M, Morrice, J.A., Dahm, C.N., Campana, M.E. (1996). Parent lithology, surface–

1156   groundwater exchange, and nitrate retention in headwater streams. *Limnology and*

1157   *Oceanography 41*: doi: 10.4319/lo.1996.41.2.0333.

1158   Warburton, J. (1996). Active braidplain width, bed load transport and channel morphology

1159   in a model braided river. *Journal of Hydrology (New Zealand)*, 35(2), 259–285.

1160   http://www.jstor.org/stable/43944775

1161   Ward, A.S. (2015). The evolution and state of interdisciplinary hyporheic research. *WIREs*

1162   *Water 3*: 83-103, doi:10.1002/wat2.1120

1163   Ward, A.S., Packman, A.I. (2019). Advancing our predictive understanding of river corridor

1164   exchange. *WIREs Water 6*: doi:10.1002/wat2.1327

1165   White, D.S. (1993). Perspectives on defining and delineating hyporheic zones. *Journal of the*

1166   *North American Benthological Society 12*: pp. 61– 69.

1167   White, P.A., Kovacova, E., Zemansky, G., Jebbour, N., Moreau-Fournier, M. (2012).

1168   Groundwater-surface water interaction in the Waimakariri River, New Zealand, and

1169   groundwater outflow from the river bed. *Journal of Hydrology (NZ) 51*: 1-23.

1170   Wöhling, T., Gosses, M.J., Wilson, S.R., Davidson, P. (2018). Quantifying river–groundwater

1171   interactions of New Zealand's gravel-bed rivers: The Wairau Plain. *Groundwater, 56*: 647–

1172   666, doi:10.1111/gwat.12625

1173   Wöhling, T., Wilson, S.R., Wadsworth, V., Davidson, P. (2020). Detecting the cause of change

1174   using uncertain data: Natural and anthropogenic factors contributing to declining

1175   groundwater levels and flows of the Wairau Plain aquifer, New Zealand. *Journal of*

1176   *Hydrology: Regional Studies 31*:100715, doi:10.1016/j.ejrh.2020.100715

1177   Wu, G.D., Shu, L.C., Lu, C.P., Chen, X.H., Zhang, X. Appiah-Adjei, E.K., Zhu, J.S. (2015).

1178   Variations of streambed vertical hydraulic conductivity before and after a flood season.

1179   *Hydrogeology Journal 23*: 1603-1615 doi:10.1007/s10040-015-1275-9

1180   Wu, F.-C & Huang, H.-T. (2000). Hydraulic Resistance Induced by Deposition of Sediment in

1181   Porous Medium. *Journal of Hydraulic Engineering 126 (7)*: 547-551

1182   Zhou, Y., Ritzi, R.W., Soltanian, M.R., Dominic, D.F. (2014). The influence of streambed

1183   heterogeneity on Hyporheic flow in gravelly Rivers. *Groundwater 52*: 206–216,

1184   doi:10.1111/gwat.12048